

Metal Injection Moulding of Inconel 718 using a Water Soluble Binder System

Andrew Ben Hales



**The
University
Of
Sheffield.**

**A thesis submitted in fulfilment of the requirements for the degree of
Master of Philosophy in the Department of Material Science and
Engineering**

The University of Sheffield

(July 2015)

Abstract

Inconel 718 components are typically cast or machined from solid in various industries. The properties of Inconel 718 make the processing of small complex parts very difficult.¹⁻⁴ There is an emerging interest in metal injection moulding (MIM) of Inconel 718.⁵⁻¹¹

MIM is a manufacturing process best used for the batch production of small complex components. The process involves mixing fine metal powders with a series of binder components to produce a pelletised feedstock. This feedstock can then be processed using an injection moulding machine to produce moulded parts. The parts then need to be solvent debinded and then sintered close to the melting temperature to fully densify the metal powder.

Polyethylene glycol (PEG) is a common component of water soluble feedstock for metal injection moulding. The processability of Inconel 718 MIM feedstocks using PEG with varying molecular weight was investigated in this work.

Inconel 718 powder was formulated with different molecular weight PEG, poly (methyl methacrylate) (PMMA) and stearic acid (SA) to produce a homogenous pelletized feedstock. The powder loading for each feedstock as well as the concentration of PMMA and SA were unchanged for the entirety of this work, the only variable being the molecular weight of PEG used.

The rheological behaviour of each of these feedstocks was analysed to determine injection moulding parameters and stability. Investigations into the mouldability of tensile bar components, differential scanning calorimetry (DSC) characteristics as well as debinding behaviour were all carried out.

Parts were sintered and heat treated with density and dimensional measurements taken throughout, in order to identify the effect of PEG molecular weight on the different processing steps.

Metallography and mechanical testing was carried out to compare the properties of each feedstock with industrial standards.

One of the key findings from this work was that the molecular weight of PEG used had an effect on the debinding time of the moulded parts. Parts moulded from a higher molecular

weight PEG require a longer period of time in a water bath in order to achieve 100% weight loss.

It was found that a debinding temperature of 40°C produces sintered parts with a higher density, compares with debinding at 50°C or 60°C.

There was no trend in sintered density across the different molecular weights of PEG, when the same debinding temperature was used. This was the same for the mechanical testing results, which showed no clear trend across the range of parts.

The mechanical properties of the injection moulded tensile bars exceed the properties of AMS 5383 (for cast specimens) and are inferior to AMS 5662 (wrought specimens).

The mechanical properties are also currently inferior to that of MIM standard AMS 5917, however HIP'ing of the components could improve the mechanical strength and this could result in the standards being met.

Table of Contents

Abstract.....	2
List of Figures	7
List of Tables	10
1. Introduction and Aims	11
2. Literature Review.....	12
2.1. Inconel 718.....	12
2.1.1. Chemical and Physical Properties	12
2.1.2. Heat Treatment of Inconel 718.....	13
2.1.3. MIM of Inconel 718.....	13
2.2. MIM Powders.....	14
2.2.1. Atomising Techniques	14
2.2.1.1. Gas Atomisation	14
2.2.1.2. Water Atomisation.....	15
2.2.2. Powder Characteristics	16
2.2.2.1. Effect of Powder Size	16
2.2.2.2. Effect of Powder Morphology.....	17
2.3. The Metal Injection Moulding Process	17
2.3.1. Introduction	17
2.3.2. Binder Systems.....	18
2.3.3. Mixing.....	21
2.3.4. Injection Moulding.....	22
2.3.5. Debinding.....	24
2.3.6. Sintering.....	25
3. Experimental Procedure	29
3.1. Introduction	29
3.2. Materials	29

3.2.1.	Inconel 718.....	29
3.2.2.	Binder components.....	29
3.3.	Production of Feedstock.....	30
3.3.1.	Feedstock Recipe	30
3.3.2.	Mixing.....	31
3.3.3.	Pelletisation.....	32
3.4.	Rheology	34
3.5.	Injection Moulding of Tensile Bars	34
3.6.	Dimensional and Density Measurements of Moulded Samples.....	36
3.7.	Recycling of Feedstock.....	36
3.8.	Water Debinding.....	37
3.9.	Sintering	37
3.10.	Dimensional and Density Measurements of Sintered Samples.....	39
3.11.	Heat Treatment.....	39
3.12.	Dimensional and Density Measurements of Heat Treated Samples	41
3.13.	Metallography of All Samples	41
3.14.	Tensile Testing.....	44
4.	Experimental Results and Discussion.....	46
4.1.	Materials	46
4.1.1.	Inconel 718.....	46
4.1.2.	Binder components.....	47
4.2.	Rheology	49
4.3.	Injection Moulding of Tensile Bars	54
4.4.	Water Debinding.....	58
4.5.	Sintering	68
4.6.	Dimensional and Density Measurements of Sintered Samples.....	68
4.7.	Heat Treatment.....	71

4.8.	Dimensional and Density Measurements of Heat Treated Samples	72
4.9.	Microstructure Investigation	73
4.10.	Tensile Testing.....	75
5.	Conclusions	78
6.	References	79

List of Figures

Figure 2.1 Turbocharger component manufactured by GKN Sinter Metals ²⁰	14
Figure 2.2 Secondary electron microscopy image showing the morphology of gas atomised 316L stainless steel ²⁷	15
Figure 2.3 Z-blade mixer (left) and a twin screw extruder (right) ^{48,49}	21
Figure 2.4 Arburg ALLROUNDER 270C injection moulding machine ⁵⁰	22
Figure 2.5 The injection moulding cycle ⁵¹	23
Figure 2.6 Schematic of powder sintering evolution of MIM components ²⁵	26
Figure 2.7 Part progression: moulded part (left), debinded part (middle) and sintered part (right) ⁵⁵ (sintered part height = 25mm)	26
Figure 2.8 Batch sintering furnace (TAV H5) ⁵⁶	28
Figure 3.1 Malvern Mastersizer 3000	29
Figure 3.2 Perkin Elmer Pyris 6 DSC	30
Figure 3.3 Pelletised Inconel 718 feedstock after being extruded twice by the Arburg Injection Moulding Machine, using the Sheffield binder system recipe	33
Figure 3.4 Rosand RH2000 Malvern capillary rheometer	34
Figure 3.5 Die cavity for MIM tensile test piece ⁵⁷	35
Figure 3.6 Thermal debinding and sintering profile for Inconel 718	38
Figure 3.7 Mettler Toledo New Classic Archimedes scale	39
Figure 3.8 Solution treatment and ageing profile for Inconel 718 in accordance with AMS 5917 -11. 40	
Figure 3.9 Cut position for mounted tensile bars	41
Figure 3.10 Struers Tegramin-20 grinding and polishing machine	41
Figure 3.11 Nikon Eclipse LV150 microscope	43
Figure 3.12 Zwick/Roell Z050 tensile testing machine	44
Figure 3.13 Extensometer camera image showing how the specimens were clamped	45
Figure 4.1 Particle size distribution of the Inconel 718 powder.	46
Figure 4.2 Secondary electron image of the Inconel 718 powder used in this work ⁶	47
Figure 4.3 DSC trace for PEG 1500, showing the onset and endset of the peak	49
Figure 4.4 Rheology of PEG 1500 Inconel 718 feedstock.....	50

<i>Figure 4.5 Rheology of PEG 4000 Inconel 718 feedstock.....</i>	<i>50</i>
<i>Figure 4.6 Rheology of PEG 6000 Inconel 718 feedstock.....</i>	<i>51</i>
<i>Figure 4.7 Rheology of PEG 8000 Inconel 718 feedstock.....</i>	<i>51</i>
<i>Figure 4.8 Rheology of PEG 10000 Inconel 718 feedstock.....</i>	<i>52</i>
<i>Figure 4.9 Rheology of PEG 12000 Inconel 718 feedstock.....</i>	<i>52</i>
<i>Figure 4.10 Rheology of PEG 20000 Inconel 718 feedstock.....</i>	<i>53</i>
<i>Figure 4.11 Line gradient for each PEG for rheology measured at 120°C.....</i>	<i>53</i>
<i>Figure 4.12 Inconel 718 sample moulded using PEG 1500 flat part showing powder separation (injection point on left hand side of image)</i>	<i>54</i>
<i>Figure 4.13 Injection moulded tensile bar using PEG 20000</i>	<i>58</i>
<i>Figure 4.14 The effect of water temperature on the debinding rate PEG 1500 feedstock.....</i>	<i>58</i>
<i>Figure 4.15 The effect of water temperature on the debinding rate PEG 4000 feedstock.....</i>	<i>59</i>
<i>Figure 4.16 The effect of water temperature on the debinding rate PEG 6000 feedstock.....</i>	<i>59</i>
<i>Figure 4.17 The effect of water temperature on the debinding rate PEG 8000 feedstock.....</i>	<i>60</i>
<i>Figure 4.18 The effect of water temperature on the debinding rate PEG 10000 feedstock.....</i>	<i>60</i>
<i>Figure 4.19 The effect of water temperature on the debinding rate PEG 12000 feedstock.....</i>	<i>61</i>
<i>Figure 4.20 The effect of water temperature on the debinding rate PEG 20000 feedstock.....</i>	<i>61</i>
<i>Figure 4.21 Defects caused to PEG 1500 parts during debinding at 60°C.....</i>	<i>62</i>
<i>Figure 4.22 The effect of PEG molecular weight on the debinding time at 40°C.....</i>	<i>63</i>
<i>Figure 4.23 The effect of PEG molecular weight on the debinding time at 50°C.....</i>	<i>63</i>
<i>Figure 4.24 The effect of PEG molecular weight on the debinding time at 60°C.....</i>	<i>64</i>
<i>Figure 4.25 ln(1/F) plot to show two stage debinding mechanism for PEG 1500 at 40°C.....</i>	<i>64</i>
<i>Figure 4.26 ln(1/F) plot to show two stage debinding mechanism for PEG 1500 increasing water temperatures.....</i>	<i>65</i>
<i>Figure 4.27 ln(1/F) plot to show dissolution mechanism for PEG 1500 at increasing water temperatures.....</i>	<i>66</i>
<i>Figure 4.28 ln(1/F) plot to show dissolution mechanism for PEG 6000, PEG 12000 and PEG 20000 at 40°C.....</i>	<i>67</i>
<i>Figure 4.29 Part density after sintering for each debinding temperature.....</i>	<i>70</i>

Figure 4.30 Inconel 718 tensile bars for PEG 20000, as moulded (left), debinded (middle) and sintered (right) 71

Figure 4.31 Optical micrograph of Inconel 718 PEG 2000 sample; (a) and (b) as sintered, (c) and (d) after solution treatment and ageing as per AMS 5917 -2011..... 74

Figure 4.32 0.2% proof stress and ultimate tensile strength of tested samples..... 76

Figure 4.33 MIM of Inconel 718 0.2% P.S and UTS in comparison with industrial standards 77

List of Tables

<i>Table 2.1 Chemical Composition specification of Inconel 718 in accordance with AMS 5917-2011</i> ¹⁹	12
<i>Table 2.2 Required Attributes for a MIM binder system</i> ²⁵	18
<i>Table 2.3 The University of Sheffield Binder System for MIM</i>	20
<i>Table 2.4 Debinding classification and techniques</i> ²⁵	24
<i>Table 2.5 Sintering process effects (adapted from German²⁵)</i>	27
<i>Table 3.1 Feedstock recipe used for each molecular weight of PEG</i>	31
<i>Table 3.2 Feedstock mixing regime used for each PEG</i>	32
<i>Table 3.3 Arburg extrusion settings for MIM of Inconel 728</i>	33
<i>Table 3.4 Injection moulding parameters for MPIF ISO 2740 tensile bars</i>	36
<i>Table 3.5 Thermal debinding and sintering cycle for Inconel 718</i>	38
<i>Table 3.6 Solution treatment profile for Inconel 718</i>	40
<i>Table 3.7 Ageing profile for Inconel 718</i>	40
<i>Table 3.8 Grinding and Polishing method for Inconel 718 samples</i>	42
<i>Table 3.9 Glycerigia composition and application</i>	43
<i>Table 4.1 Particle size distribution parameters of Inconel 718 gas atomised powder</i>	47
<i>Table 4.2 Melting point range for PEG determined by DSC</i>	48
<i>Table 4.3 Injection moulding settings of Inconel 718 feedstock used for moulding of tensile bars</i>	55
<i>Table 4.4 Injection moulded dimensions and weight for all feedstocks</i>	57
<i>Table 4.5 Trend line gradient for PEG 6000, PEG 12000 and PEG 20000 for dissolution and diffusion stage of water debinding</i>	67
<i>Table 4.6 Average dimensions, shrinkage and density changes after sintering</i>	69
<i>Table 4.7 Inconel 718 density comparison of sintered and heat treated tensile bars using different molecular weight PEG</i>	72
<i>Table 4.8 Inconel 718 solution treated and aged mechanical properties of tensile bars</i>	75

1. Introduction and Aims

The University of Sheffield has been using a well-established binder system for MIM feedstocks for a number of years.^{2,7,12-15} This system has three parts, comprising of; PEG (83 wt %), PMMA (15 wt %) and SA (2 wt %). The molecular weight of PEG typically used is PEG 1500.

The injection moulding process can be challenging when using feedstocks formulated from PEG 1500. The high fluidity of PEG 1500 at higher temperatures can cause separation of the metal particles and the binder, resulting in parts that contain voids or a poor surface finish. PEG 1500 feedstock also has a higher cooling time in the mould after injection. The injection moulded parts also have a weak structure and can easily be broken during ejection from the mould tool, or transportation.

The molecular weight of PEG will have an overall effect on the processing properties of the feedstock, in terms of; mouldability, cooling time after injection, part strength after moulding, debinding time and temperature required as well as, part stability and strength during debinding. The aim of this work is to measure and evaluate these factors by mixing different feedstocks.

2. Literature Review

2.1. Inconel 718

Inconel 718 is a nickel-based superalloy mainly used for demanding, high temperature applications in the aerospace, petrochemical, automotive and nuclear industry. ^{2,16}

Inconel 718 is typically produced by forging as well as ingot casting, followed by investment casting. However, production via these methods often produce undesirable side-effects, such as; elemental segregation, formation of laves, white-spots and freckles, rough surface finish and low dimensional accuracy. ^{6,9,17,18}

2.1.1. Chemical and Physical Properties

Inconel 718 is a precipitation-hardenable nickel-chromium alloy; the chemical composition of this alloy in accordance with AMS 5917-2014 for Metal Injection Moulded Nickel Based Alloy 718 parts can be seen in Table 2.1.

Table 2.1 Chemical Composition specification of Inconel 718 in accordance with AMS 5917-2011 ¹⁹

Element	min	max
Carbon (3.1.4)	--	0.08
Manganese	--	0.35
Silicon	--	0.35
Phosphorus	--	0.015
Sulfur	--	0.015
Chromium	17.00	21.00
Nickel	50.00	55.00
Molybdenum	2.80	3.30
Columbium (Niobium)	4.75	5.50
Titanium	0.65	1.15
Aluminum	0.20	0.80
Cobalt	--	1.0
Tantalum (3.1.3)	--	0.05
Boron	--	0.006
Copper	--	0.30
Lead (3.1.3)	--	0.0005 (5 ppm)
Bismuth (3.1.3)	--	0.00003 (0.3 ppm)
Nitrogen (3.1.4)	--	0.02
Oxygen (3.1.4)	--	0.06
Selenium (3.1.3)	--	0.0003 (3 ppm)
Iron	remainder	

Components produced from Inconel 718 are typically cast or machined from solid. Inconel 718 is in general very difficult to machine because of the following aspects ²;

- Elevated temperature strength
- High hardness (30 – 40 Rockwell C)
- High work hardening rates
- Low thermal diffusivity leading to high temperatures during machining
- Presence of highly abrasive carbide particles due to tool wear

2.1.2. Heat Treatment of Inconel 718

For the majority of applications and industries, Inconel 718 is specified as a solution treated and aged alloy. ³

Solution treating is a heat treatment process that produces uniformly dispersed particles (precipitates) within the microstructure of the alloy. The precipitates improve the microstructure by hindering the movement of dislocations and therefore improving strength.

^{3,4}

Inconel 718 is hardened by the formation of aluminium, titanium and niobium and is induced by heat treating in a temperature range of 600°C – 815°C. In order for these precipitates to form correctly, the ageing constituents must be solution annealed at 930°C - 1010°C, followed by a rapid cooling, plus precipitation hardening at 1720°C for 8 hours, furnace cool to 620°C and hold for 18 hours, followed by air cooling to room temperature. ^{3,6}

2.1.3. MIM of Inconel 718

There is an emerging commercial interest in the MIM of nickel based superalloys such as Inconel 718. This interest has largely been driven by the automotive and aerospace industries, for the production of complex components capable of working at high temperature.⁹ Figure 2.1 shows an Inconel 718 turbocharger component currently manufactured using MIM by GKN Sinter Metals (www.gkn.com/sintermetals). The MIM feedstock and conditions for processing these parts has not been revealed.

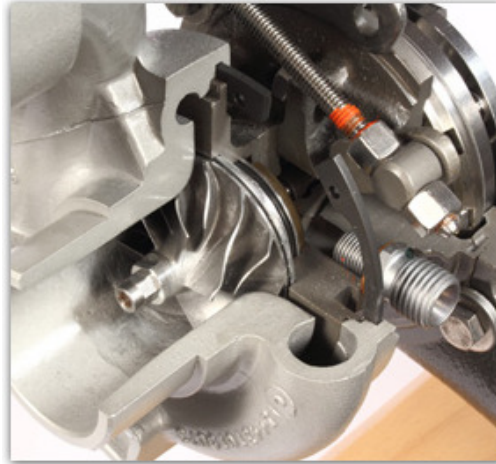


Figure 2.1 Turbocharger component manufactured by GKN Sinter Metals ²⁰

2.2. MIM Powders

2.2.1. Atomising Techniques

2.2.1.1. Gas Atomisation

The processing technique for producing metal powders by gas atomisation begins with the melting of a metal or alloy by induction (or other heating process), followed by forcing the melt through a nozzle. After the liquid metal passes through the nozzle, it is struck with a high velocity flow of gas. The gas breaks the melt into fine droplets; which, during free-fall from the nozzle, solidify into small spherical droplets. ²¹⁻²³

A number of gases can be used to atomise the melt, including; nitrogen, argon, helium or air. Air is suitable for some powders; however particles that are atomised in air typically show a high surface oxidation. This may not be suitable for materials that will be difficult to reduce during sintering.

The gas atomisation process is best adopted for speciality powders where spherical powder size is required, as the process naturally produces spherical droplets that remain spherical as they solidify before landing. This is a useful property for a number of processes as spherical powders generally flow more easily than other shapes. This is because there is less locking together of particles, which helps where movement is needed, for example in additive manufacturing, powder pressing and MIM. ^{22,24,25}

The use of inert gas during the gas atomisation makes the process as a whole quite costly, compared with other methods. The process requires a more complex system, resulting in a higher capital and running costs.²⁶

Figure 2.2 shows a typical Scanning Electron Microscope (SEM) image of a gas atomised powder. Particles produced from this process can be seen to have a high spherical uniformity and also have a high surface purity and a high packing density.

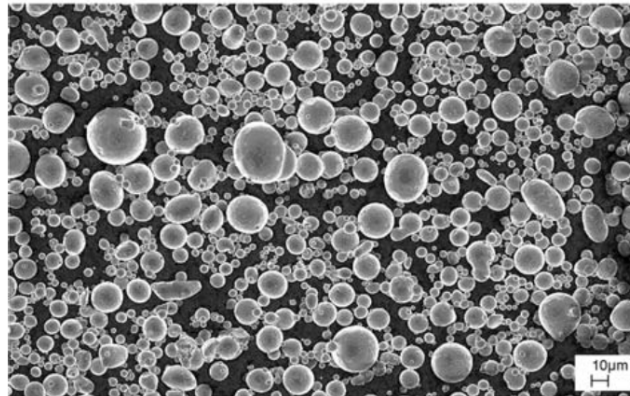


Figure 2.2 Secondary electron microscopy image showing the morphology of gas atomised 316L stainless steel²⁷

2.2.1.2. Water Atomisation

An alternative method is water atomisation where a stream of molten metal is struck with a high velocity spray of water. The water pressure can be increased/decreased to respectively change the size of the particles produced from the process. The water atomisation process yields irregular shaped particles with a rough surface. The solidification of the metal powders occurs quickly after impact with the jet of water resulting in the metal particles having a turbulent and irregular shape, as they are not allowed to cool naturally and form rounded shapes.^{7,22,24,28}

When used in MIM feedstocks, the irregular shaped particles produced from water atomised powders can inhibit feedstock flow during injection moulding.²⁵ However Kipphut and German (1991) reported that injection moulded parts produced from water atomised powder have better shape retention because of increased interlocking between irregular shaped particles, as compared to spherical particles produced from gas atomisation.²⁹

Figure 2.3 shows a typical Scanning Electron Microscope (SEM) image of a water atomised powder.

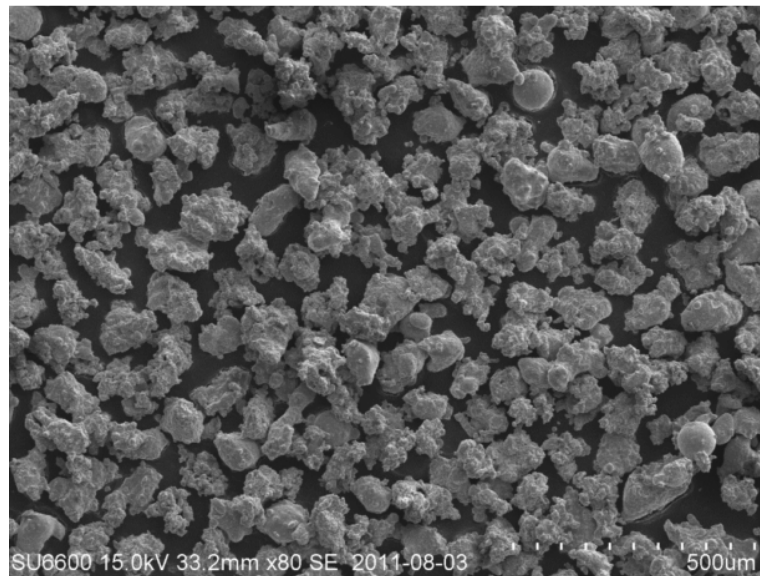


Figure 2.3 Secondary electron image showing the morphology of water atomised 316L stainless steel³⁰

2.2.2 Powder Characteristics

2.2.2.1 Effect of Powder Size

Metal powders for conventional powder metallurgy applications can be commercially obtained with typical sizes in the range of 20µm – 200µm.^{15,25}

For the purpose of MIM, finer powders are required to ensure suitable flow behaviour and rapid sintering. However there are conflicting opinions amongst professionals with regards to the optimum particle size and distribution.

Martyn suggests that particle sizes up to 45µm could be used for the MIM process.³¹ The same opinion is shared by Hartwig who states that if powders were used with a size greater than 45µm, there would be an inherent lack of sintering activity.²²

An alternative view is that the mean particle size should remain below 8µm when moulding parts with a sintered weight of 75g or less. Powders with a greater particle size should be used when moulding heavier parts, this would allow the green part to perform better during the debinding stage.³²

German also agrees that the best mean particle size for the MIM process should be between $2\mu\text{m}$ - $8\mu\text{m}$.²⁵ Using fine powders within this range generally allows sintering to occur more readily due to a greater surface area between particles. Using finer powders would also yield a greater finished part density.²⁵ The disadvantage of using fine powders would be the difficulty in handling. For example additional safety precautions would need to be taken to prevent inhalation of powders during mixing.

2.2.2.2. Effect of Powder Morphology

The shape of metal powders can have a significant effect on the final properties of the sintered MIM part. Powder shape can also affect flow characteristics during moulding.^{28,33-36}

German explains that spherical powders are widely preferred in MIM because of the high packing densities that can be achieved in the injection moulding process.²⁵ There is also reduced inter-particle friction giving the feedstock better flow characteristics, as compared to irregular shaped particles.²⁹

2.3. The Metal Injection Moulding Process

2.3.1. Introduction

Metal injection moulding (MIM) is becoming a widely exploited and cost effective manufacturing technology for the production of complex components in a variety of metallic materials.

MIM is a manufacturing process that involves the manipulation of fine metal powders, so that they flow and can be processed using technology developed for polymers. This is achieved through mixing metal powders with a series of polymer/wax binders, to form a feedstock.¹⁵ The feedstock produced can be processed by an injection moulding machine, which would conventionally be used for plastics. Parts produced from the injection moulding process are subjected to further process steps to remove the polymer from the part, followed by a sintering operation to fully densify the metal particles. Standard heat treatment processes, machining, plating or anodising can be applied to the part where necessary after sintering.

2.3.2. Binder Systems

The role of the binder system within MIM feedstock is to transport the fine metal particles into the mould cavity, to form the required part shape. The binder must then solidify to allow the part to be ejected from the mould without fracture and be able to withstand handling and transportation for further process steps.

Most binder systems are comprised of multiple components, in order to deal with the conflicting requirements within the MIM process. For example, one component of the binder system makes the mixture fluid at elevated temperatures to allow injection. Other components in the binder act as a “backbone” to ensure the part is transportable after debinding and stable during sintering. Small additions of surfactants or wetting agents are added to coat the metal particles ensuring a more homogenous feedstock.

Some of the required binder attributes can be found in Table 2.2.

Table 2.2 Required Attributes for a MIM binder system²⁵

Powder Interaction
<ul style="list-style-type: none">• Low contact angle with powder• Good adhesion with powder• Chemically passive (non-reactive with powder)
Flow Characteristics
<ul style="list-style-type: none">• Low viscosity (< 10 Pa/s) at mould tool temperature• Fast cooling after injection• Rigid after cooling
Debinding
<ul style="list-style-type: none">• Multiple components with different characteristics• Non-corrosive and non-toxic during decomposition• Decomposition above moulding and mixing temperatures
Commercial
<ul style="list-style-type: none">• Inexpensive and commercially available• Long shelf life• Non-degradable

Binder systems for MIM can be categorised into two groups; wax based binders and polymer based binders.²⁴

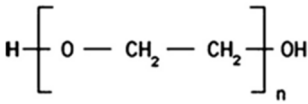
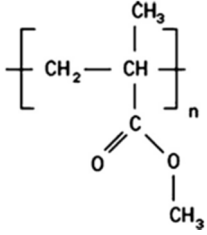
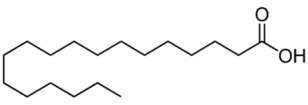
Work was carried out by Mobellegh et al into the use of a paraffin wax based binder system for the injection moulding of copper.³⁷ The binder system also included polyethylene and stearic acid as a backbone binder and surfactant respectively. The work found that the main advantages of a wax based binder system is the ease of processing the feedstock, combined with a short solvent debinding time. However, there are issues when using wax based binders during mould ejection and part handling. Parts are considered far more delicate and as a consequence, proper location and sizing of ejector pins for part ejection and a good surface finish of mould tool are required.³⁸

According to work carried out by Adames, polymer based binder systems have several advantages over wax based systems.²⁴ This includes better flow characteristics and part strength after moulding, the possibility of sequential debinding and better shape retention during debinding.

Polymer binder systems based on a water soluble polymer provide an economical advantage over polymers requiring liquid or gaseous nitric acid as the debinding solvent.³⁹ The use of common debinding solvents such as nitric acid can be flammable, carcinogenic and not environmentally acceptable. Water soluble feedstock for MIM is now commercially available from a number of suppliers in a range of materials. These companies include PolyMIM⁴⁰ and Ryer Incorporated.⁴¹

The binder system developed by The University of Sheffield also contains a water soluble polymer. This binder system is comprised of three parts; Polyethylene Glycol (PEG), poly (methyl methacrylate) (PMMA) and stearic acid (SA). Further details of this binder system can be seen in Table 2.3.

Table 2.3 The University of Sheffield Binder System for MIM

Polymer	Purpose	Removal Process	Binder Weight %	Chemical Structure
PEG <i>(Polyethylene Glycol)</i>	Provides fluidity during injection.	Water debinding	83%	 42
PMMA (emulsion) <i>(poly (methyl methacrylate))</i>	Backbone binder to retain part shape and strength during/after water debinding.	Thermal debinding	15%	 43
SA <i>(stearic acid)</i>	Surfactant in the binder system to wet the metallic powder and prevent agglomeration.	Thermal debinding	2%	 44

The PEG used in this binder system has a molecular weight of 1500 g/mol (grams per mole). The molecular mass is determined by the sum of the total mass in grams of all the atoms that make up a molecule per mole. The molecular weight of PEG is determined by the number of ethylene glycol units included in each polymerised molecule of PEG, and which varies from 300 g/mol to 10,000,000 g/mol. The molecular weight in turn determines the characteristics of each type of PEG. In general, the average molecular weight of PEG used for MIM feedstocks is between 400 and 2000 g/mol.⁴⁵

The fairly open, short chained helical structure of PEG 1500 has been preferred by The University of Sheffield, because of the polymer's low melting temperature (38-54°C)¹⁵ and its high solubility in water. However, lower molecular weight PEGs have a very low viscosity

at low temperatures, resulting in a significant drawback during the injection moulding process. The use of PEG 1500 for the moulding of large or very complicated components can be very challenging due to this low viscosity. It is important to fill the mould as quickly as possible to prevent the feedstock from cooling, however when using a high injection pressure, powder-binder separation can occur.

2.3.3. Mixing

The mixing process for MIM feedstock is an important factor. Inconsistencies that are present in the feedstock cannot be rectified in the latter processing steps. The feedstock produced must be homogenous, with all the metal powder being uniformly dispersed throughout the chosen binder.

Work carried out by Supati et al has shown that feedstocks processed under different mixing conditions will result in the subsequent feedstock having different rheological properties. Work has also shown that the results of an inconsistent feedstock can include moulding defects such as cracks, voids and part distortion.⁴⁶

The mixing of feedstocks should take place above the melting temperature of the binder constituents to ensure the metal particles within the feedstock are sufficiently coated.^{46,47}

There are various mixing methods employed by the MIM industry. As previously mentioned, the main aim of the mixing process is to ensure a homogenous feedstock. Examples of these mixing methods include the z-blade mixer and twin screw extruders. Figure 2.3 shows a schematic of both of these methods.

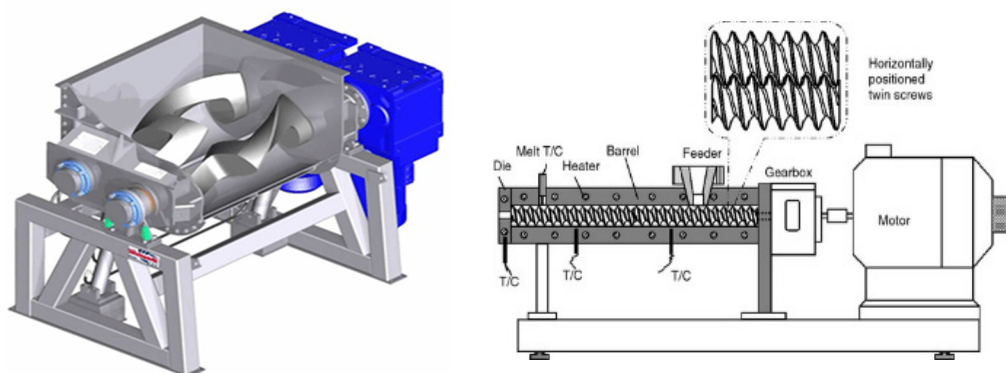


Figure 2.3 Z-blade mixer (left) and a twin screw extruder (right)^{48,49}

Non-contact mixing machines are often used on a smaller, laboratory scale for the production of MIM feedstock. These machines work by the spinning of a high speed arm in one direction. A container located at the end of this arm rotates in the counter direction. This dual asymmetric centrifuge mechanism relies on the friction created between particles, to heat and melt the feedstock into a homogenous mixture.

2.3.4. Injection Moulding

The aim of the injection moulding process is to convert the pelletized/granulated feedstock into a required part geometry, through the process of heating, injection and cooling. Injection moulding is considered a mass production process due to the repeatability and speed of the method.²⁵ Figure 2.4 shows a typical injection moulding machine, supplied by Arburg GmbH.



Figure 2.4 Arburg ALLROUNDER 270C injection moulding machine⁵⁰

The MIM feedstock is transported through a screw and barrel unit which mixes, compresses and heats the feedstock, ready for injection.

The heated feedstock is then injected under high pressure into a mould cavity, allowing the feedstock to flow through and fill the cavity to achieve the required geometry. After injection

the part is allowed to cool and solidify in the mould cavity. The mould cavity then opens and the part is ejected. The mould tool closes and the injection process can then begin again.

The injection moulding cycle comprises the following stages;

- Mould closing: The two halves of the mould tool close and a clamping pressure is applied
- Injection: Melted feedstock that has been heated by the barrel unit is injected into the mould cavity by the advance of the reciprocating screw.
- Packing: The screw and barrel unit imparts pressure onto the mould cavity to compensate material shrinkage, prevent counter flow, fully fill the cavity and prevent holes/porosity.
- Cooling and plasticising: the part is allowed to cool inside the closed mould tool. The binder constituents plasticize and stiffen to produce a solid part. During the cooling time, the screw rotates and melts material for the next part.
- Ejection: The clamping force is released and the two halves of the tool separate. The now solid part is ejected from the mould via ejector pins.

A schematic of the injection moulding cycle showing the relative duration of each stage can be found in Figure 2.5.

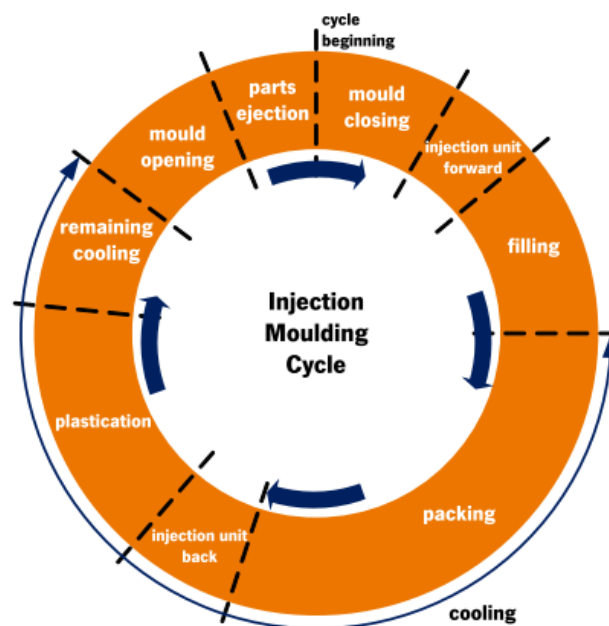


Figure 2.5 The injection moulding cycle ⁵¹

Compared to the injection moulding of polymers, flow rates for MIM feedstocks need to be quite high to allow the feedstock to completely fill the mould tool, this is because the presence of fine metal particles in the feedstock inhibit the flow of the polymers during injection. The presence of metal powders dramatically increases the thermal diffusivity of the feedstock, meaning that a longer cooling time is required compared to plastic injection moulding.

The ejected part is an oversized component comprising the metal powder plus polymer/wax binder; this is known as the “green” part.

2.3.5. Debinding

As previously mentioned the main role of the binder system is to facilitate the injection moulding of the part. After the “green” part is formed, the majority of the binder must be removed in order to proceed with the sintering operation. Failure to remove the binder before sintering will result in part distortion, cracking and possible contamination.⁵¹ Following the debinding process, the part is referred to as the “brown” part.

Depending on the binder system used, there are several debinding techniques adopted by the MIM process. These techniques are subdivided into thermal and solvent extraction and can be seen in Table 2.4.

Table 2.4 *Debinding classification and techniques*²⁵

Thermal Debinding	Solvent Debinding
Evaporation	Extraction
Degradation	Supercritical
Wicking	Condensation
Catalytic	

Thermal debinding techniques involve the slow heating of part in a reducing or inert atmosphere, inside an oven/furnace to provide a progressive degradation of the binder. Flowing gas during the process helps remove the binder in its now gaseous form, as well as keeping the oven/furnace surfaces clean.^{52 53}

The thermal debinding technique is often adopted because of its simplicity, as a low investment is required and there is no processing and recycling of any liquid waste. The downside of the process is the longer processing times and tendency of the debinded parts to distort.⁵¹

The solvent debinding method involves the use of a solvent, either as a liquid or a vapour to remove binder from the part. This process is comprised two stages. The first stage of the process dissolves the binder from the surface of the part. This initial step leaves a porous structure at the surface only. The solvent can then access the surface pores and further binder is diffused by capillary action from the body of the part.⁵⁴ The disadvantage of using the solvent debinding process is the difficulty in handling and disposing of the hazardous liquids/gases.

Water and organic solvents such as hexane, toluene, pentane, heptane, methylchloride and acetone can be used to absorb the binder, leaving behind an open porous structure of metal particles and backbone binder. The network of pores left by the solvent debinding process allows the backbone binder to be more readily removed during a later thermal debinding process. Parts are typically submersed in these liquids for a period of time (12 - 24 hours typical) and at a certain temperature (20°C - 60°C typical) in order for this removal to occur.

2.3.6. Sintering

The aim of the sintering process is to densify the “brown” debinded part through the elimination of pores, to create a near dense finished part. The process involves heating the parts up to near the melting point of the material, allowing the metal particles to sinter together. At a high enough temperature cohesive necks form between metal particles where there is sufficient contact. Figure 2.6 shows the sintering action of powder during the sintering process.

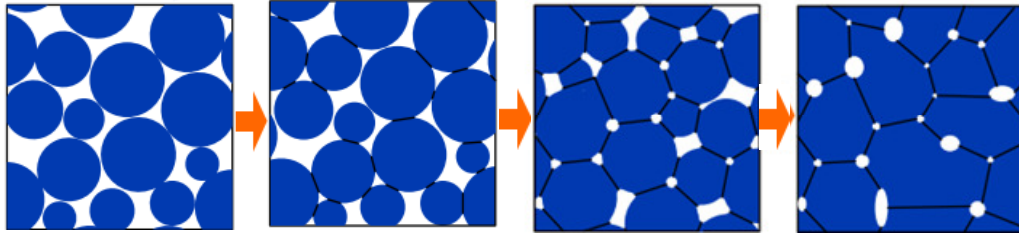


Figure 2.6 Schematic of powder sintering evolution of MIM components ²⁵

Different sintering rates and shrinkages can be seen between different particle sizes and shapes. For example, parts with a smaller particle size will sinter together faster as the surface area per unit volume would be greater, and therefore the energy to drive the process. Particles with irregular shape will sinter differently depending on the contact between particles, and in this case, maintaining a highly uniform shrinkage will also be difficult. ²⁵

Figure 2.7 shows the part progression from a moulded, debinded and sintered part. There is often little to no difference in appearance from the moulded and debinded part.



Figure 2.7 Part progression: moulded part (left), debinded part (middle) and sintered part (right) ⁵⁵ (sintered part height = 25mm)

Table 2.5 evaluates the advantages and disadvantages of some of the process variables during sintering.

Table 2.5 Sintering process effects (adapted from German²⁵)

Change to aid sintering	Effects
Decrease in particle size	Faster sintering
	Greater expense
	Higher impurity level
	Increased hazards
Increase in sintering time	Greater expense
	Grain growth
	Reduced productivity
Increase in temperature	Greater shrinkage
	Grain growth
	Greater expense
	Furnace limitations
	Pore coarsening
Increase in packing density	Less shrinkage
	Less binder
	Slower debinding

Sintering provides the interparticle bonding to achieve the required mechanical, physical and surface properties. The higher the density achieved, the more likely the sintered part is to achieve the required mechanical properties. It is difficult for MIM components to compete

on a like for like basis with wrought and machined material properties, because 100% density is not achieved. However, in general the properties achieved by MIM are enough to satisfy most applications and can be further improved through Hot Isostatic Pressing (HIP).

Atmosphere is an important aspect in the sintering of MIM components, several factors must be considered. After debinding the MIM component still contains a residual backbone binder that must be extracted by the sintering atmosphere prior to densification of the part. Failure to do this can result in carbon sooting of the furnace as well as carbon contamination of the sintered component.²⁵

During sintering most metals require protection from atmospheric oxidation. Surface oxides hinder the bonding of particles and can result in lower mechanical and physical properties.

Sintering in a vacuum furnace is a popular method, as most metallic materials can be processed in vacuum. The process is clean, reproducible and avoids a low partial pressure of oxygen which results in oxide reduction. Depending on the alloy, it can be beneficial to run a slight pressure of inert gas such as argon or helium to prevent element depletion during sintering.

Pure hydrogen is a preferred atmosphere for stainless steels because it inhibits oxidation better than an inert or vacuum only cycle. Hydrogen also improves the surface finish and quality of a variety of materials. Figure 2.8 shows a typical batch sintering furnace with a front opening loading door. This furnace is capable of high vacuum and different sintering atmospheres including argon, helium, hydrogen, and nitrogen.



Figure 2.8 Batch sintering furnace (TAV H5)⁵⁶

3. Experimental Procedure

3.1. Introduction

This chapter outlines the experimental methods used for the comparative study of the effect of using different molecular weight PEG in MIM feedstocks. The adopted strategy was to produce a range of feedstocks from the PEG available, where possible and appropriate keeping processing parameters the same, to reduce variability in results.

3.2. Materials

3.2.1. Inconel 718

The Inconel 718 powder used for this work was supplied by Sandvik Osprey Ltd (UK) and was produced by inert gas atomisation, yielding spherical powder. The particle size distribution for the supplied Inconel 718 powder was determined using the particle size laser analyser, Malvern Mastersizer 3000 (shown in Figure 3.1).



Figure 3.1 Malvern Mastersizer 3000

3.2.2. Binder components

The thermal properties of the range of PEG plus the PMMA was performed in order to understand the melting points of each. Differential Scanning Calorimetry (DSC) was carried out on a Perkin Elmer Pyris 6 DSC, under argon atmosphere with a heating rate of 5°C/min. (shown in Figure 3.2)

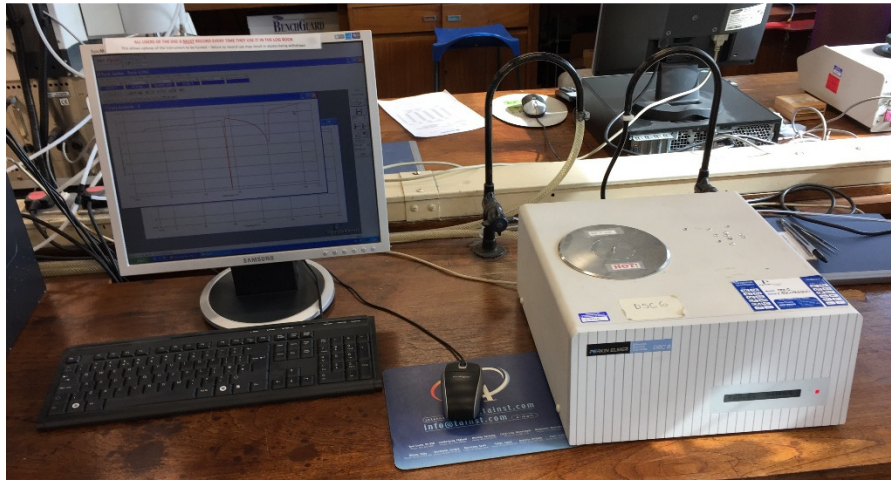


Figure 3.2 Perkin Elmer Pyris 6 DSC

3.3. Production of Feedstock

3.3.1. Feedstock Recipe

As previously mentioned, the University of Sheffield binder system comprises 83 wt% PEG, 15 wt% PMMA and 2 wt% SA. This recipe was adopted for the entirety of this work and has been the foundation of work carried out by the university in the past.^{6,7,12,15}

The chosen powder loading was 59% by volume. This was chosen as an attempt to ensure the feedstocks containing a higher PEG molecular weight, would be able to flow and produce good parts during injection moulding.

The recipe shown in Table 3.1 was used for each of the seven feedstocks mixed. It was decided to mix 2kg of each feedstock, as this would be sufficient for all further experimentation. All weight measurements were taken a laboratory weighing scales, capable of results to three decimal places.

Table 3.1 Feedstock recipe used for each molecular weight of PEG

Component	Weight (g)
Inconel 718 powder	1961.1
PEG *	165.7
PMMA (emulsion)	29.7
SA	3.3

* Molecular weight of PEG used has negligible effect on density and therefore weight used in recipe

3.3.2. Mixing

Feedstock mixing was carried out on a SpeedMixer Dual Axial Centrifuge (DAC) 5000. The weighed feedstock, excluding the PMMA emulsion, was transferred to the SpeedMixer tin and mixed in five stages as described in Table 3.2. The machine was paused between each stage and the tin removed from the machine. This allowed the inner walls of the tin to be manually cleaned with a pallet knife. The PMMA emulsion was added to the tin after the third stage of mixing. This was to allow the feedstock from the first three stages of mixing to get hot enough for the addition of PMMA, which has a higher melting temperature. The same mixing regime was used for each feedstock, containing different molecular weight PEG.

Table 3.2 Feedstock mixing regime used for each PEG

Stage	Speed (rpm)	Time (s)	Components Mixed
1	400	120	IN718, PEG, SA
2	400	120	IN718, PEG, SA
3	500	120	IN718, PEG, SA
4	600	60	IN718, PEG, SA, PMMA
5	600	60	IN718, PEG, SA, PMMA

After the last stage of mixing, the feedstock was transferred on to a flat acrylic board (500mm x 500mm) and spread out thinly with a pallet knife. Each feedstock was then transferred to a laboratory oven, set to 30°C for 24 hours allowing any water in the feedstock to evaporate.

3.3.3. Pelletisation

Mixed feedstock must be pelletised so that it can be fed into the hopper of the injection moulding machine. The pellets should be as small as possible; ideally no greater than 2mm in diameter and 2mm in length. This is to allow the feedstock to be fed into the screw and barrel in the most constant manner possible.

After 24 hours in the laboratory oven, the feedstock was broken into small pieces and fed into the hopper of the Arburg 270C Allrounder machine. The machine was used in manual mode to heat and extrude the feedstock into a string, followed by cutting the feedstock into small pellets.

To promote homogeneity, the feedstock was extruded through the injection moulding machine twice. This was found adequate to produce a smooth flowing feedstock. The extrusion temperature and speed settings used for each of the feedstocks is given in Table 3.3.

Table 3.3 Arburg extrusion settings for MIM of Inconel 728

Code	Representation	Setting
T801	Temperature zone 1 (hopper)	90°C
T802	Temperature zone 2	130°C
T803	Temperature zone 3	135°C
T804	Temperature zone 4	140°C
T805	Temperature zone 5 (nozzle)	150°C
v403	Rotational speed	5 rpm
p403	Back pressure	10 bar

The resulting pelletised feedstock can be seen in Figure 3.3.



Figure 3.3 Pelletised Inconel 718 feedstock after being extruded twice by the Arburg Injection Moulding Machine, using the Sheffield binder system recipe

3.4. Rheology

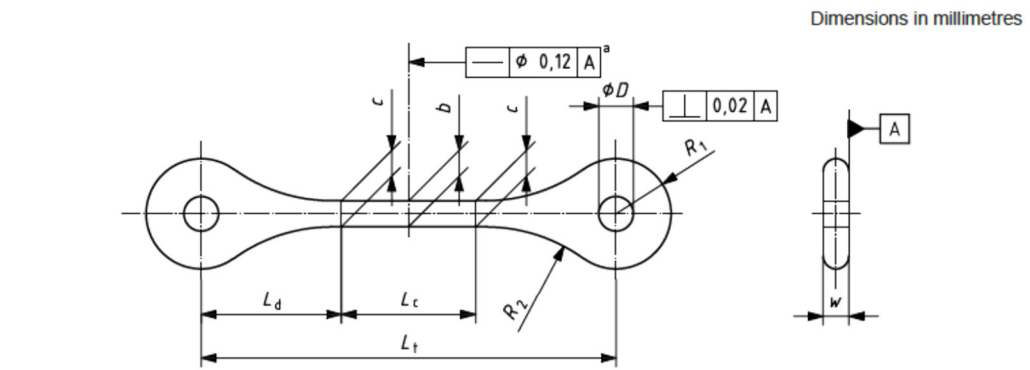
The rheological characterisation of different feedstocks was carried out using a Rosand RH2000 Malvern capillary rheometer (shown in Figure 3.4). The capillary length was 16mm and diameter 1.5mm. The feedstock was heated up to various temperatures and the capillary rheometer imparted a controlled force on the material, at controlled speeds through a set of dies. The pressure required to push the material through the 1.5mm diameter hole is measured. The rheometer varies the speed at which the material is pushed out, in order to simulate different shear rates during the moulding cycle. Viscosity is sensitive to shear rate, so the information gathered was used to optimise the injection moulding process.



Figure 3.4 Rosand RH2000 Malvern capillary rheometer

3.5. Injection Moulding of Tensile Bars

Tensile bars in accordance with MPIF ISO 2740:2009, Type A2 (sintered metal materials, excluding hardmetals- tensile test pieces), were injection moulded using an Arburg 270C Allrounder machine. Figure 3.5 shows the schematic dimensions and shape of the required mould cavity (not moulded or sintered dimensions).



^a Applies to gauge length L_c .

Type	b	c	L_c	L_d	L_t	w	R_1	R_2	D
	$\pm 0,1$	$\pm 0,1$	$\pm 0,2$	$\pm 0,2$	$\pm 0,5$	0,1	$\pm 0,5$	$\pm 0,5$	$\pm 0,1$
A1	$\varnothing 5,82$	$\varnothing 5,87$	30,5	31,75	94	5,85	R 25	R 38	$\varnothing 7,85$
A2	$\varnothing 3,8$	$\varnothing 3,85$	30,5	27,5	85,5	3,85	R 23	R 23	$\varnothing 6$

Figure 3.5 Die cavity for MIM tensile test piece ⁵⁷

The initial moulding parameters for the tensile bars are outlined in Table 3.4. Visual, dimensional and weight measurements was carried out after each injection to ensure parts were uniform and defect free. The mould tool was kept at 21°C for each of the different feedstocks used.

Table 3.4 Injection moulding parameters for MPIF ISO 2740 tensile bars

Temperature Profile		Parameters			
Barrel zone 1	90	Part volume	8.5 cm ³		
Barrel zone 2	130	Switch over volume	3.5 cm ³		
Barrel zone 3	135	Cooling time	45 seconds		
Barrel zone 4	145	Back pressure	20 bar		
Barrel zone 4	150				
Injection Profile		Packing Profile			
Injection pressure	800 bar		Stage 1	Stage 2	Stage 3
Injection speed	10 cm ³ /s	Hold pressure	800 bar	800 bar	25 bar
		Time	0.5	0.25	0.25

3.6. Dimensional and Density Measurements of Moulded Samples

After a good part was moulded, dimensional and weight checks were recorded using a pair of digital callipers (results to two decimal places) and a set of laboratory scales (results to three decimal places) respectively. The criteria for an acceptable part was one that contained no visible surface defects, cracks or under filling, no visible powder separation on the surface and a clean and a clean break from the filling point of the mould.

3.7. Recycling of Feedstock

The runners and sprue produced with every injection moulded part were fed back into the hopper with the unused “virgin” feedstock and re-used. This is not expected to influence the

experimentation, as the temperatures used for injection did not exceed the melting temperatures for any of the binder constituents.

3.8. Water Debinding

Components were solvent debound in a water bath at a set temperature and time. The optimal temperature and time for the water debinding was determined by a series of experiments, measuring the weight of PEG lost at a set time over a range of temperatures. Three samples from each feedstock were used in the experimentation for each of the three temperatures used for water debinding.

The experiments were carried out at water temperatures of 40°C, 50°C and 60°C. Parts were removed from the water bath, allowed to dry for 24 hours and then weighed. This process continued hourly and a graph was plotted to determine the debinding rate and time for each temperature. The experiment was carried out for a total debinding time of 15 hours, with hourly increments of submersion to begin with. As the percentage of PEG remaining was minimal, large time increments of submersion were used.

The parts were placed on a perforated aluminium tray to ensure good contact with the surrounding water.

3.9. Sintering

Parts were sintered in a Centorr VI MIM vacuum furnace (shown in figure 3.3), capable of sintering in high vacuum and in an inert argon atmosphere.

The debound parts were placed on aluminium oxide trays and stacked in the vacuum furnace. The sintering cycle included a thermal debinding process step at 350°C and 440°C in order to remove the backbone PMMA from the parts. The sintering took place at 1270°C, both thermal debinding and sintering took place under a purified argon gas flow to prevent oxidation (0.2 ppm Oxygen). The combined thermal debinding and sintering cycle detail is displayed in Table 3.5. The combined thermal debinding and sintering temperature profile can be seen in the graph in Figure 3.6.

Table 3.5 Thermal debinding and sintering cycle for Inconel 718

From (°C)	To (°C)	Rate (°C /minute)	Hold (minutes)
0	350	3	60
350	440	2	60
440	800	5	60
800	1270	5	120
1270	0	5	0

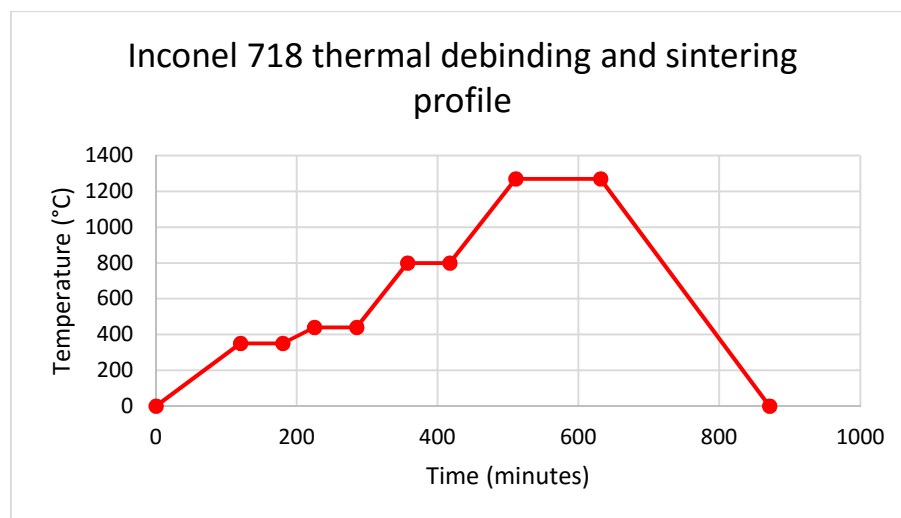


Figure 3.6 Thermal debinding and sintering profile for Inconel 718

3.10. Dimensional and Density Measurements of Sintered Samples

After the cooled parts were removed from the furnace, dimensional and weight checks were recorded using a pair of digital callipers (results to two decimal places) and a set of laboratory scales (results to three decimal places) respectively.

The density of the sintered parts was measured using a Mettler Toledo New Classic Archimedes scale, as shown in Figure 3.7 (results to three decimal places)



Figure 3.7 Mettler Toledo New Classic Archimedes scale

3.11. Heat Treatment

Heat treatment of the samples was carried out according to the solution treatment and ageing profile in AMS 5917 -2011 (Metal Injection Moulded Nickel Based Alloy 718 Parts Hot Isostatically Pressed, Solution and Aged).

The solution treatment and ageing temperature profiles are shown in Tables 3.6 and 3.7, and Figure 3.8.

Table 3.6 Solution treatment profile for Inconel 718

From (°C)	To (°C)	Rate (°C /minute)	Hold (minutes)
0	968	10	180
968	21	10	0

Table 3.7 Ageing profile for Inconel 718

From (°C)	To (°C)	Rate (°C /minute)	Hold (minutes)
21	730	10	480
730	630	1	480
630	0	10	0

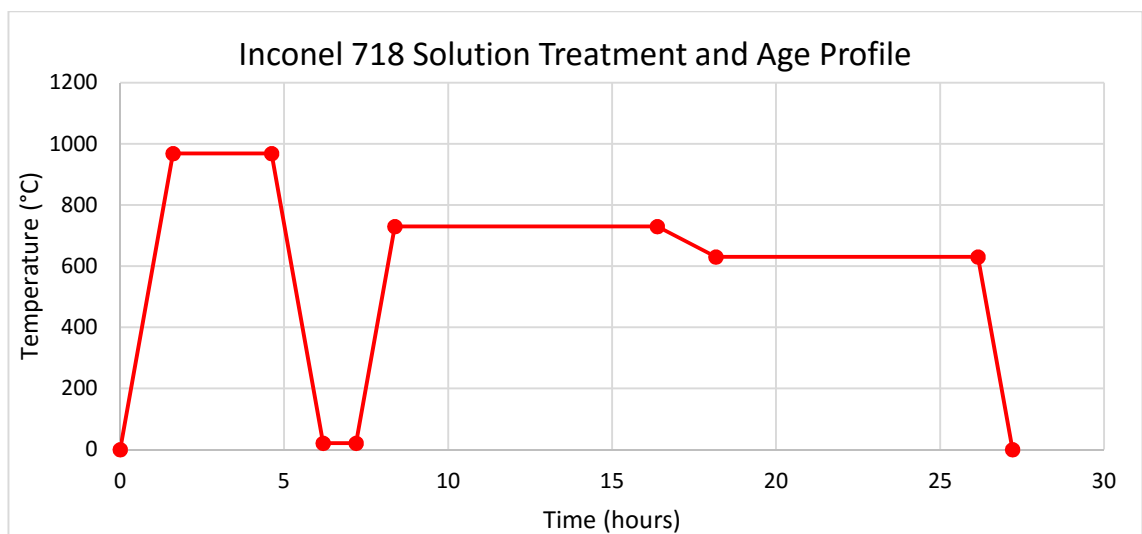


Figure 3.8 Solution treatment and ageing profile for Inconel 718 in accordance with AMS 5917 -11

3.12. Dimensional and Density Measurements of Heat Treated Samples

Dimensional, weight and density measurements for each sample were carried out using the equipment described previously.

3.13. Metallography of All Samples

Two tensile bar samples from each feedstock were taken forward for metallography, in order to discover if the molecular weight of PEG has any effect on the microstructure of the sintered and heat treated part.

Sintered and heat treated samples were sectioned using a carbide blade and mounted in Bakelite. Each sample was cut at the same position so that the metallography and porosity can be compared for each sample, as shown in Figure 3.9.



Figure 3.9 Cut position for mounted tensile bars

After mounting and identifying each sample by scribing, the parts went through a grinding and polishing procedure. A Struers Tegramin-20 machine was used as shown in Figure 3.10.



Figure 3.10 Struers Tegramin-20 grinding and polishing machine

The following procedure (Table 3.8), designed for Inconel materials and developed by the University of Sheffield, was carried out on all samples.

Table 3.8 Grinding and polishing method for Inconel 718 samples

Step	Grit Number	Time (mins)	Lubrication	Force (N)	Platen Speed (RPM)	Head Speed (RPM)	Rotational Direction
1	P180	02:00	water	25	200	70	counter-rotating
2	P240	02:00	water	25	200	70	counter-rotating
3	P500	02:00	water	25	300	70	counter-rotating
4	P600	02:00	water	25	200	70	counter-rotating
5	P1200	02:00	water	20	250	100	counter-rotating
6	P2500	03:00	water	20	300	110	counter-rotating
7	P4000	04:00	water	25	250	110	counter-rotating
8	3 μ m	03:00	Metadi 3 μ m	15	140	50	co-rotating
9	1 μ m	03:00	Diamet 1 μ m	15	140	50	co-rotating
10	MD-Chem	04:00	OP-S	15	140	60	co-rotating

All polished samples were etched in order to reveal the surface microstructure using the etchant Glycerigia. The composition of this etchant and method of application is outlined in Table 3.9.

Table 3.9 Glycerigia composition and application

Component	Volume (ml)	Ratio (%)
HCl	15	50
Glycerol	10	33
HNO ₃	5	17

** Mix fresh and use within 20 minutes, Swab sample with cotton wool for 2-3 minutes*

A Nikon Eclipse LV150 optical microscope shown in Figure 3.11, was used to examine the revealed microstructure of each heat treated sample.



Figure 3.11 Nikon Eclipse LV150 microscope

3.14. Tensile Testing

Three heat treated tensile bars from each feedstock were tensile tested in order to evaluate if PEG molecular weight has any effect on mechanical properties.

A Zwick/Roell Z050 machine was used for all tensile testing, as shown in Figure 3.12.

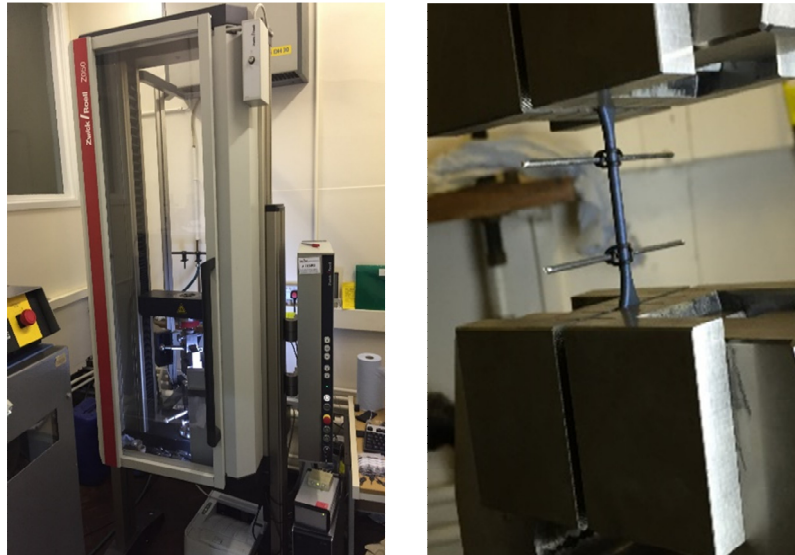


Figure 3.12 Zwick/Roell Z050 tensile testing machine

Figure 3.13 shows the configuration of tensile bars after they are loaded in between two sets of jaws. Metal rods were attached to the central portion of the tensile bar so that the extensometer camera could measure the change in gauge length during the test, removing the influence of elastic deformation of the test frame and grips. The thicker sections of the tensile bar were clamped evenly on each end, so that the tensile bars would fracture at the weakest point in the middle of the specimen.

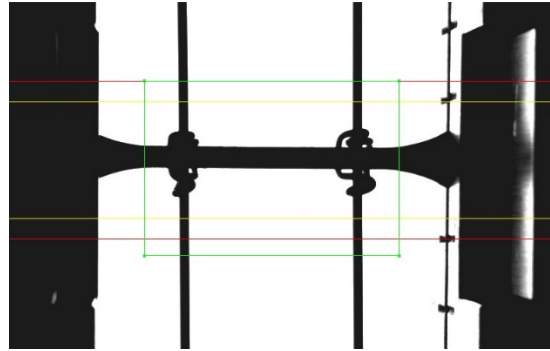


Figure 3.13 Extensometer camera image showing how the specimens were clamped

An initial load of 10N was applied before the strain was increased until the point of breaking. The strain rate was set at 0.5N/s.

The Zwick/Roell machine plotted a standard stress/strain graph until the sample fractured. This graph was then used and reinterpreted to calculate the 0.2% proof stress (0.2% PS), Young's modulus (YM) and ultimate tensile strength (UTS).

4. Experimental Results and Discussion

4.1. Materials

4.1.1. Inconel 718

Figure 4.1 and Table 4.1 illustrates the particle size distribution and parameters for the Inconel 718 powder supplied by Sandvik Osprey Ltd (UK). The measured D_{90} particle size of $15.60\mu\text{m}$ is consistent with the quoted particle size of $16.00\mu\text{m}$ provided by Sandvik. There are no measured agglomerates or larger than expected particles.

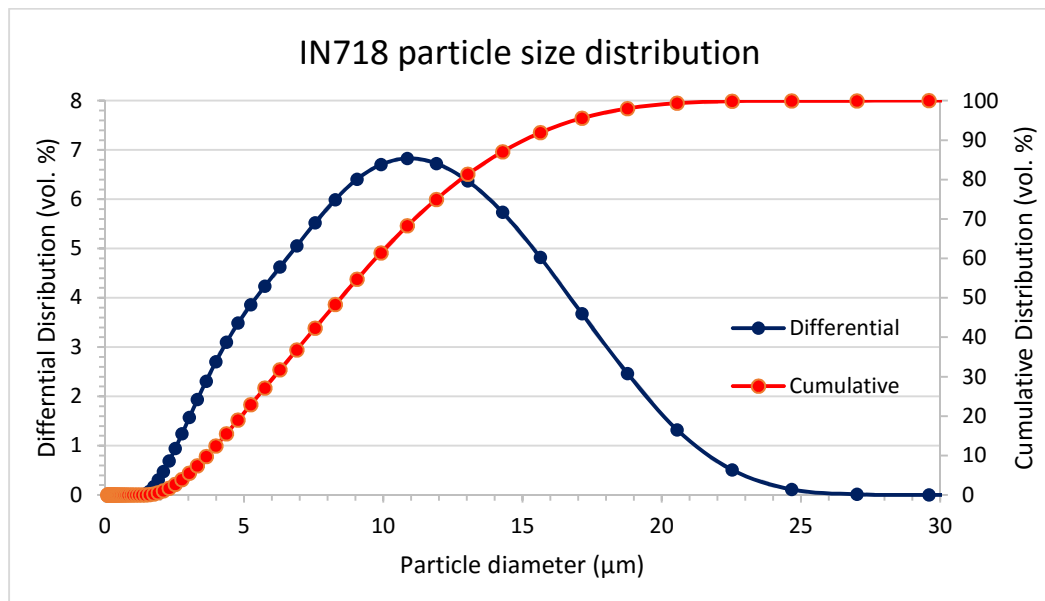


Figure 4.1 Particle size distribution of the Inconel 718 powder.

Table 4.1 Particle size distribution parameters of Inconel 718 gas atomised powder

Parameter	Value (μm)
Mean	7.87
D ₁₀	3.74
D ₅₀	8.42
D ₉₀	15.60

The morphology of Inconel 718 powder used in this work can be seen in Figure 4.2. The same batch of powder was used in previous work carried out by the university.⁶

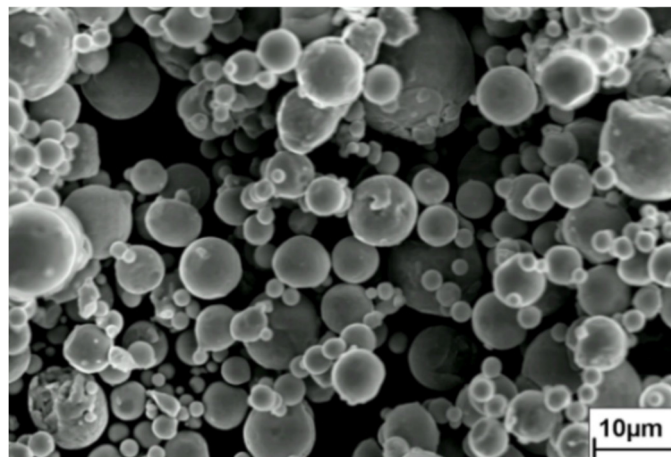


Figure 4.2 Secondary electron image of the Inconel 718 powder used in this work⁶

4.1.2. Binder components

Table 4.2 shows the DSC results for different grades of PEG used in the experimentation, as well as the PMMA. The melting range given shows the onset and endset of the peaks from the DSC graphs. PMMA was tested using DSC to determine the temperature at which it softened. It was important for further feedstock mixing and injection moulding to be above this temperature, in order to produce homogenous feedstock/parts. Figure 4.3 shows as an

example, the results from the DSC trace of PEG 1500. The onset and endset for the melting range are shown.

Table 4.2 Melting point range for PEG determined by DSC

Binder Constituent	Melting Range (°C)
PEG 1500	38 - 54
PEG 4000	44 - 56
PEG 6000	49 - 59
PEG 8000	53 - 62
PEG 10000	56 - 68
PEG 12000	59 - 72
PEG 20000	64 - 76
PMMA	118 - 135

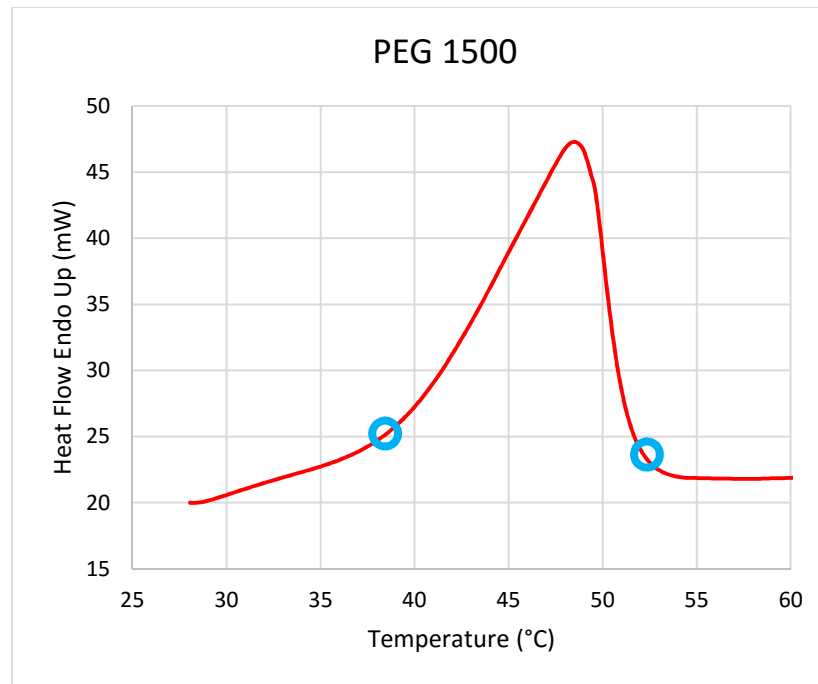


Figure 4.3 DSC trace for PEG 1500, showing the onset and endset of the peak

4.2. Rheology

It is desirable for of a MIM feedstock to behave in a pseudoplastic fashion (shear thinning), with decreasing shear viscosity with an increasing shear rate. This means that during injection (high shear) it will flow easily and fill the mould with good shape replication, and before and after the injection (low shear) the shape will be less prone to change. It is also desirable for the feedstocks to not be sensitive to processing temperature as processes may be carried out at different temperatures, and the contribution to temperature from internal frictional heating is complex and unlikely to be uniform. The results displayed in Figure 4.4–4.10, clearly show that each feedstock behaves pseudoplastically. However the sensitivity to temperature is higher with a lower molecular weight feedstock. With an increasing molecular weight, this sensitivity to temperature decreases, as shown by the graphs in Figure 4.8-4.10 for PEG 10000, PEG 12000 and PEG 20000. The temperature has little to no effect for any of the feedstocks when subjected to a low shear rate, the shear viscosity appears unaffected by change of temperature.

As was expected, the use of a high molecular weight PEG resulted in a higher shear viscosity at higher shear rates. This can be seen in Figure 4.11; where for each feedstock, the line

gradient was calculated for the data series at 120°C. The trend shows a reduction in gradient for a higher molecular weight PEG.

Higher molecular weight feedstocks are less sensitive in nature to change in temperature but have higher shear viscosity at a higher shear rate.

Figure 4.4 Rheology of PEG 1500 Inconel 718 feedstock

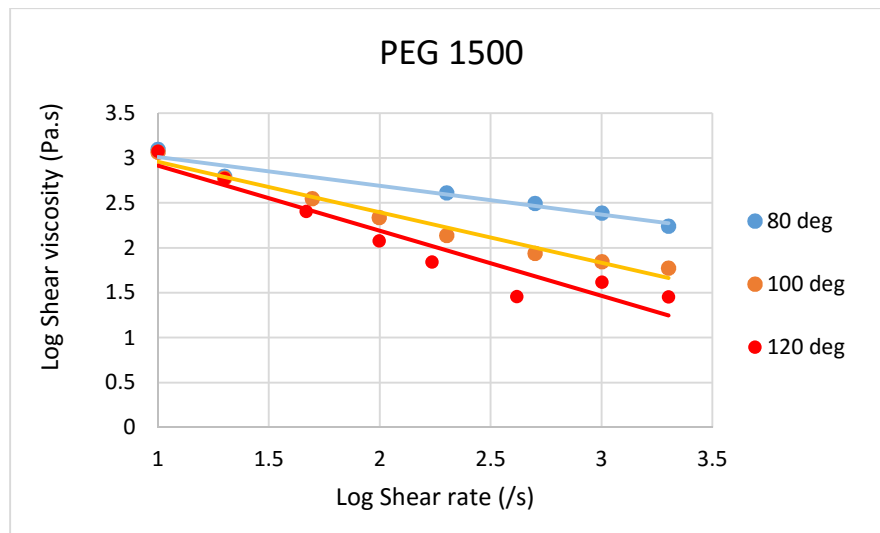


Figure 4.5 Rheology of PEG 4000 Inconel 718 feedstock

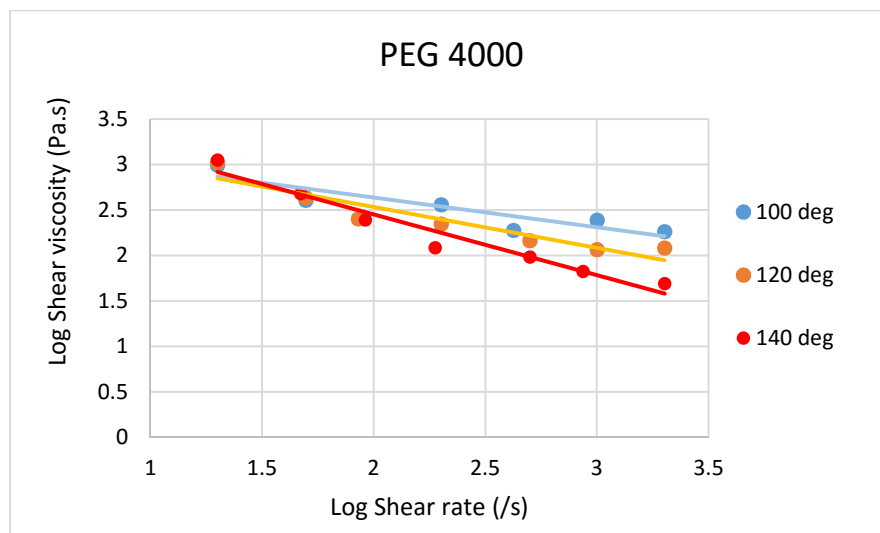


Figure 4.6 Rheology of PEG 6000 Inconel 718 feedstock

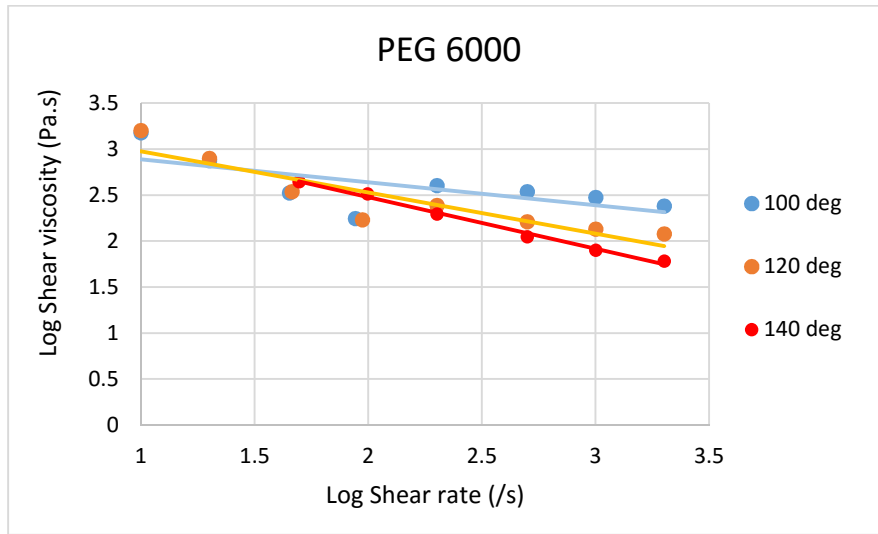


Figure 4.7 Rheology of PEG 8000 Inconel 718 feedstock

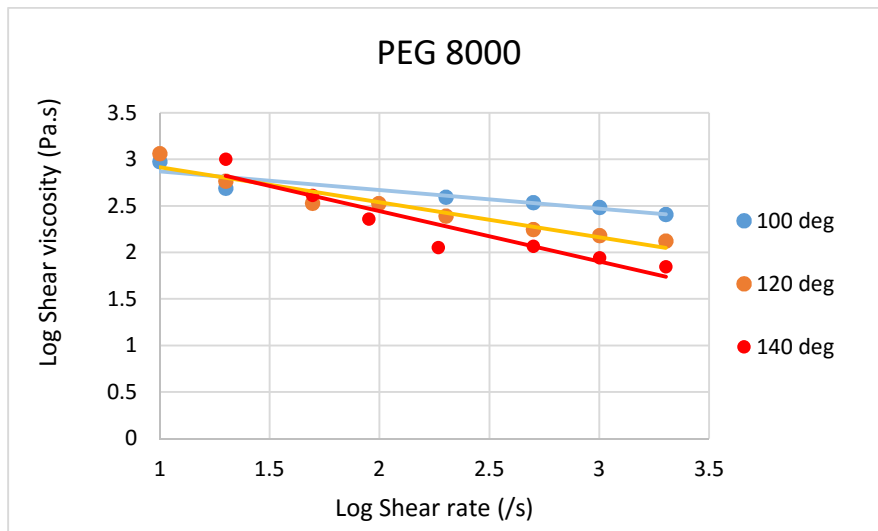


Figure 4.8 Rheology of PEG 10000 Inconel 718 feedstock

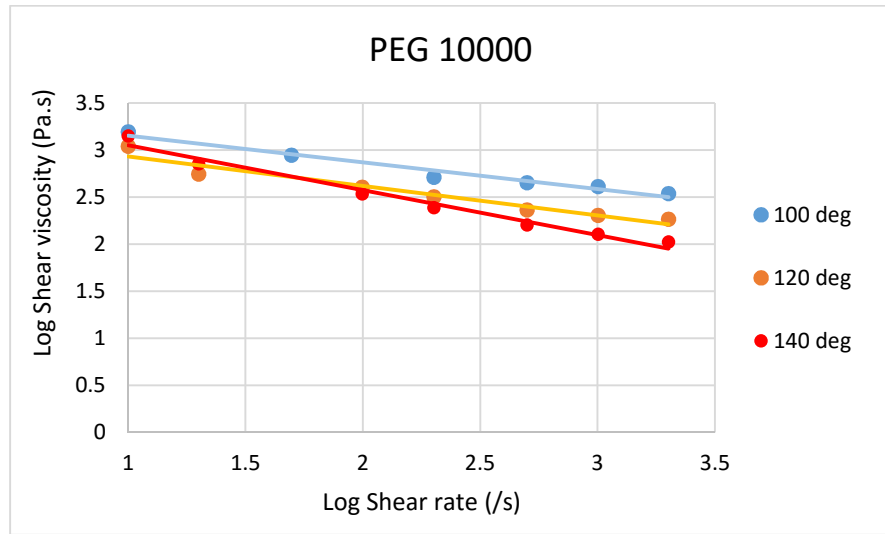


Figure 4.9 Rheology of PEG 12000 Inconel 718 feedstock

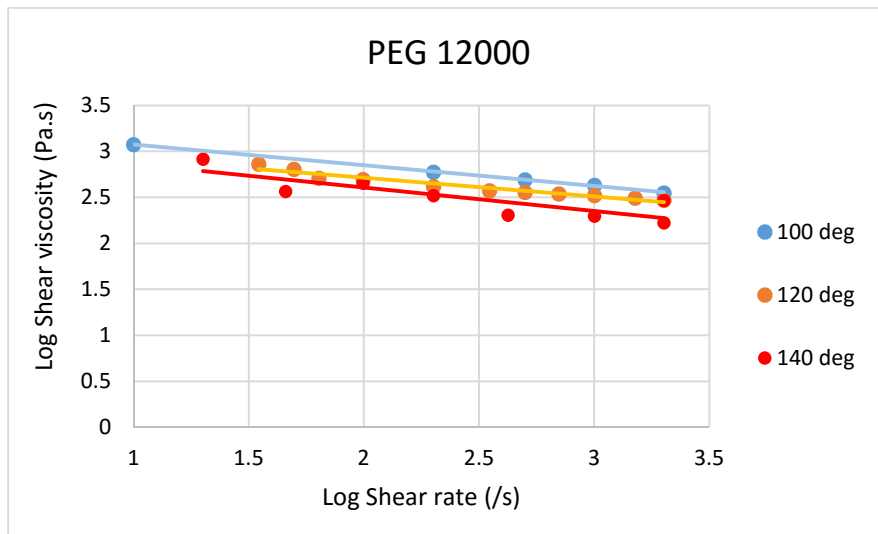


Figure 4.10 Rheology of PEG 20000 Inconel 718 feedstock

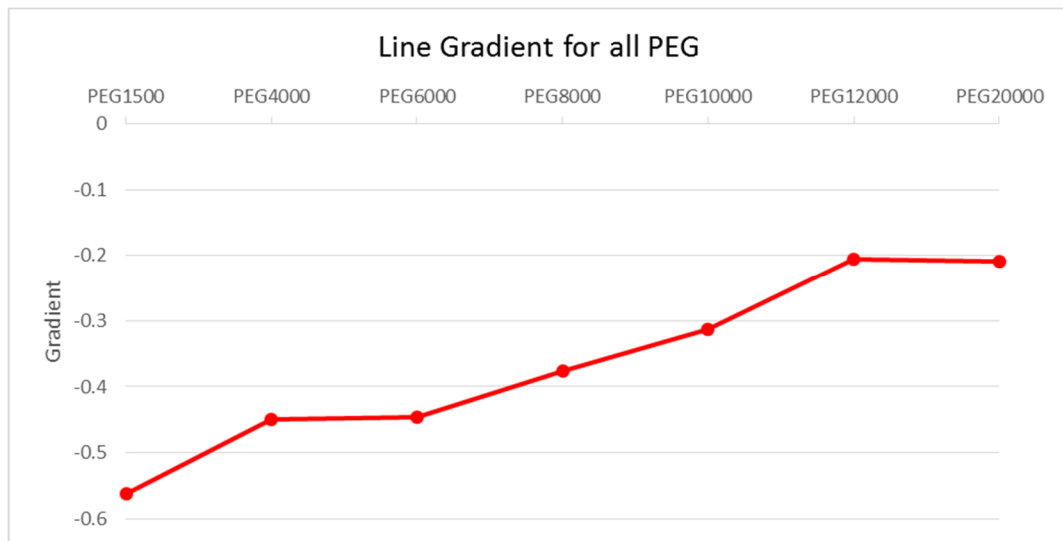
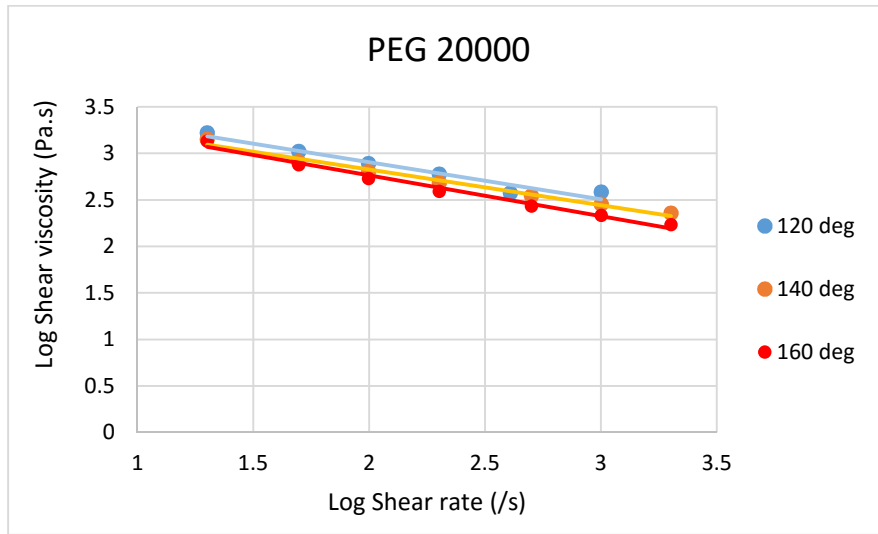


Figure 4.11 Line gradient for each PEG for rheology measured at 120°C

4.3. Injection Moulding of Tensile Bars

Tensile bars in accordance with ISO 2740:2009 were injection moulded on an Arburg 270C machine using the machine settings given in the previous chapter. The same settings were adopted for each feedstock used, however some settings were changed for different feedstocks in order to mould complete parts. In the case of PEG 1500, moulding at an injection pressure of 800 bar revealed parts with a poor surface finish, this was most likely caused by jetting of the feedstock, causing powder separation and voids.

Jetting is caused by injecting the feedstock with too much force. This results in the feedstock being sprayed into the mould cavity as opposed to the preferred gradual filling method. During jetting the metal particles that are suspended in the binder can separate, causing areas of high binder concentration with little metal. The image in Figure 4.12 shows typical parts exhibiting jetting and powder separation.

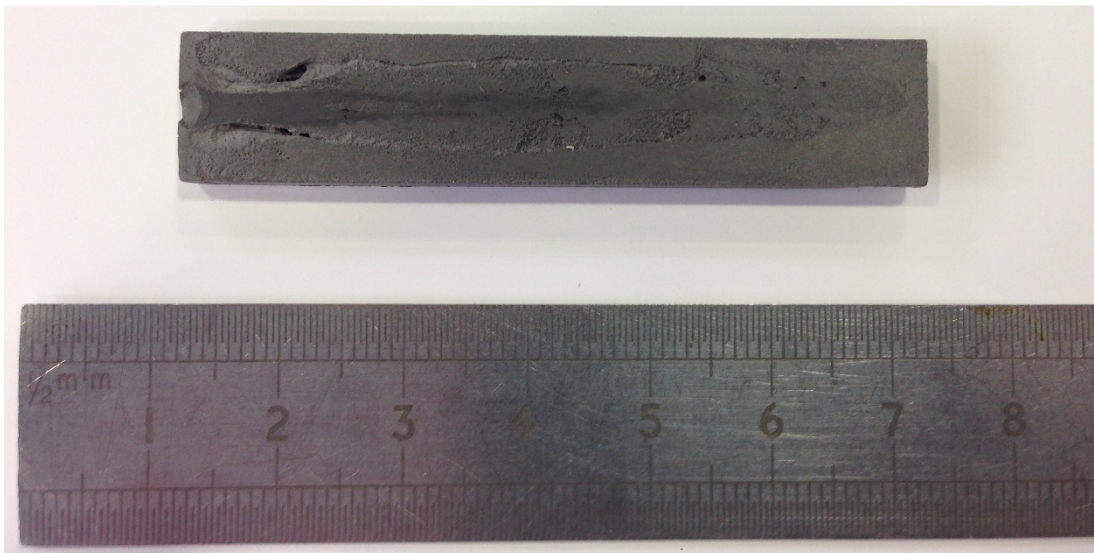


Figure 4.12 Inconel 718 sample moulded using PEG 1500 flat part showing powder separation (injection point on left hand side of image)

Full detail of the injection moulding settings used for each feedstock can be seen in Table 4.3.

Table 4.3 Injection moulding settings of Inconel 718 feedstock used for moulding of tensile bars

Parameter	PEG 1500	PEG 4000	PEG 6000	PEG 8000	PEG 10000	PEG 12000	PEG 20000
Barrel zone 1 temperature (°C)	90	90	90	90	90	90	100
Barrel zone 2 temperature (°C)	130	130	130	130	135	130	135
Barrel zone 3 temperature (°C)	135	135	135	135	140	135	145
Barrel zone 4 temperature (°C)	145	145	145	145	146	147	155
Barrel zone 4 temperature (°C)	150	150	150	150	152	155	160
Part volume (cm ³)	8.7	8.7	8.7	8.7	8.7	8.7	8.7
Switch over volume (cm ³)	3.3	3.3	3.3	3.3	3.4	3.4	3.4
Cooling time (seconds)	45	45	45	45	45	45	45
Back pressure (bar)	20	20	20	20	20	20	20
Injection pressure (bar)	625	700	700	700	750	800	850
Injection speed	10	10	10	10	10	10	10
Hold pressure stage one (bar)	625	700	700	700	750	800	850
Hold pressure stage two (bar)	625	700	700	700	750	800	850
Hold pressure stage three (bar)	25	25	25	25	25	25	25

As can be clearly seen from the injection moulding settings, the temperature of the feedstock in the barrel was increased for the higher molecular weight of PEG (PEG 10000, 12000, 20000). This increase was justified, as flowability was poor at the original temperature, resulting in incomplete and defected parts. Injection pressure and holding pressure was also increased for higher molecular weight PEG for the improvement of flowability.

As few settings as possible were changed during injection moulding between feedstocks, to reduce variability in part weight and dimensions.

After the parts were ejected from the mould tool and allowed to cool naturally, dimensional measurements and part weights were taken for each. The overall length, as well as the neck diameter of the tensile bar was taken for each part.

Table 4.4 summarises the weight and dimensional results taken from a sample range of ten parts moulded from each feedstock.

Table 4.4 Injection moulded dimensions and weight for all feedstocks

Feedstock	Average length (mm)	Average Diameter (mm)	Length σ (mm)	Diameter σ (mm)	Average weight (g)	weight σ (g)
PEG 1500	108.14	3.81	0.250	0.120	19.13	0.0825
PEG 4000	108.13	3.85	0.201	0.065	18.90	0.0834
PEG 6000	108.13	3.85	0.089	0.062	19.01	0.0346
PEG 8000	108.14	3.86	0.185	0.077	18.95	0.1030
PEG 10000	108.08	3.87	0.077	0.057	18.97	0.0275
PEG 12000	108.09	3.84	0.052	0.080	18.94	0.0394
PEG 20000	108.00	3.85	0.301	0.077	18.96	0.0492

As the results show, there is little variation or correlation between dimensions and weight measured for each feedstock, denoting the molecular weight of PEG used has little or no effect on the dimensions and weight of the moulded part. The standard deviation (shown in the above table) of part length and neck diameter is very low for each feedstock, again there is no correlation between feedstocks. There is a small variation in standard deviation between feedstocks, this must be assumed to be caused by the measuring accuracy of the callipers used for this experiment.

Figure 4.13 shows a successful moulded part from PEG 20000.



Figure 4.13 Injection moulded tensile bar using PEG 20000

4.4. Water Debinding

Water debinding experiments were carried out on injection moulded tensile bars, in order to determine the effect water temperature has on removal rate, as well as determining the debinding rate for the different feedstocks containing different molecular weight of PEG. Figure 4.14-4.20 illustrates the effect of water temperature on the debinding rates of different feedstocks.

Figure 4.14 The effect of water temperature on the debinding rate PEG 1500 feedstock

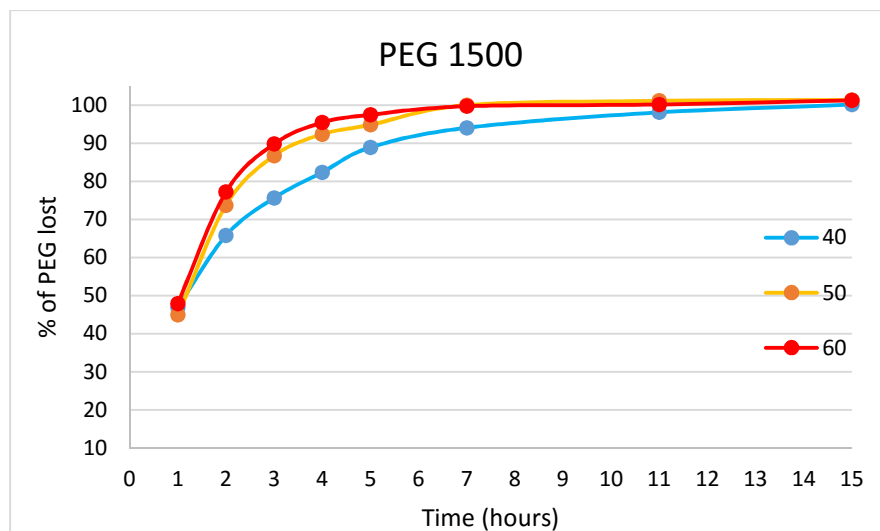


Figure 4.15 The effect of water temperature on the debinding rate PEG 4000 feedstock

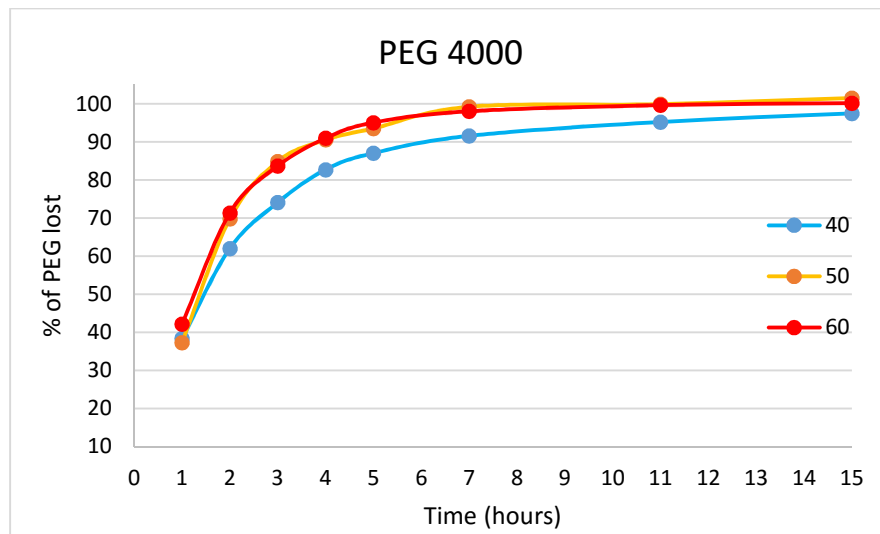


Figure 4.16 The effect of water temperature on the debinding rate PEG 6000 feedstock

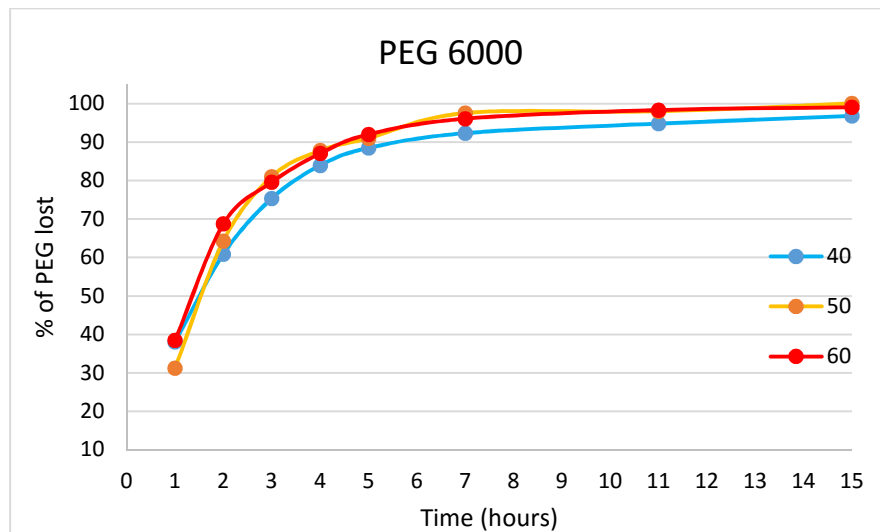


Figure 4.17 The effect of water temperature on the debinding rate PEG 8000 feedstock

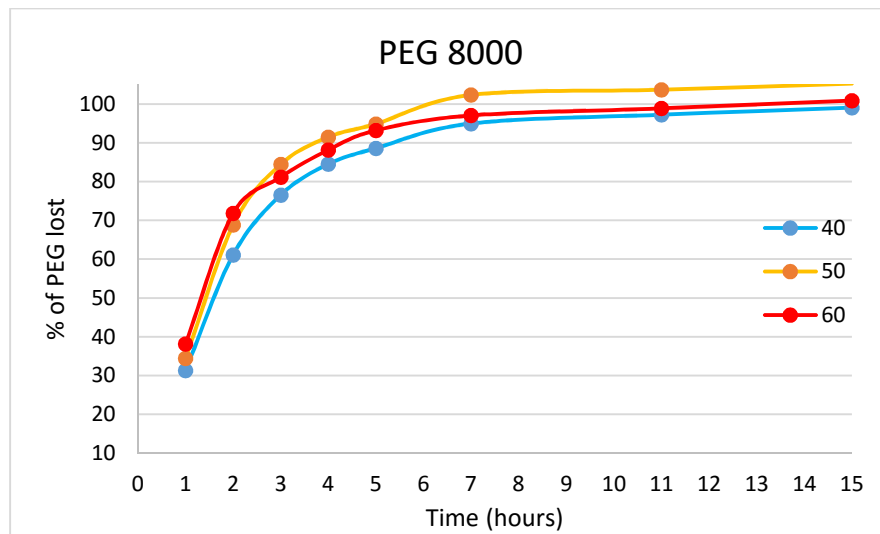


Figure 4.18 The effect of water temperature on the debinding rate PEG 10000 feedstock

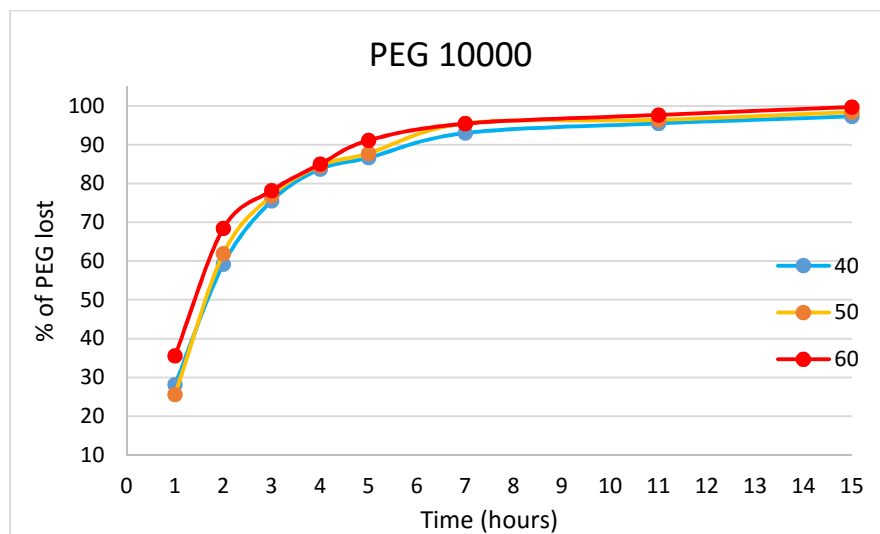


Figure 4.19 The effect of water temperature on the debinding rate PEG 12000 feedstock

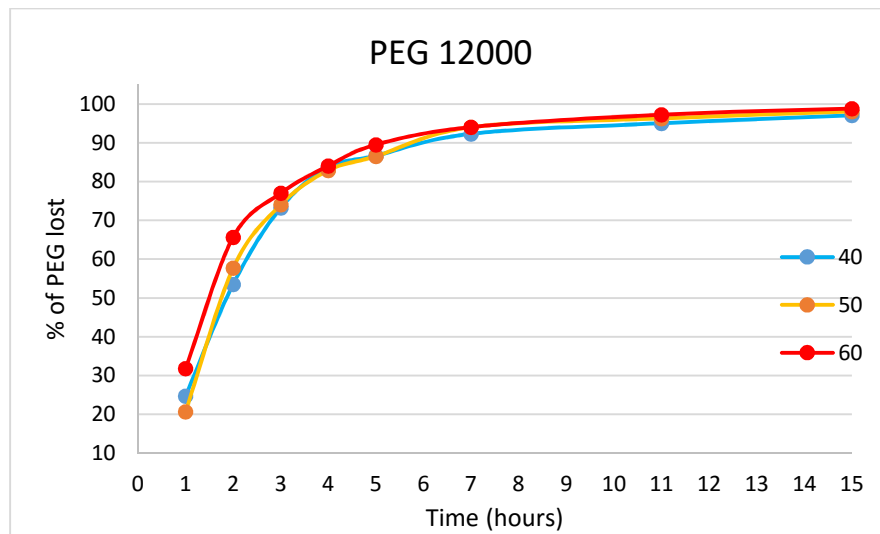
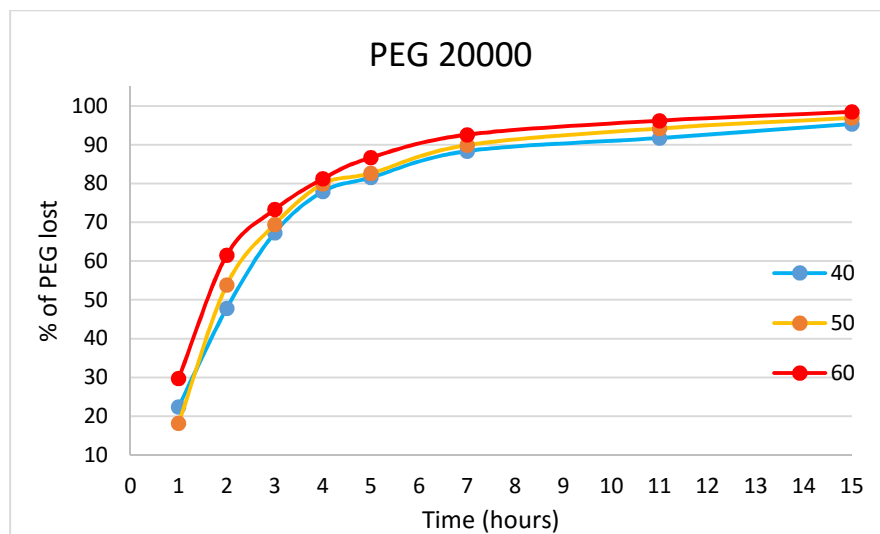


Figure 4.20 The effect of water temperature on the debinding rate PEG 20000 feedstock



The results from graphs shown in Figure 4.14-4.20 clearly indicate that, as would be expected, a higher water temperature results in an increase of the removal rate of the PEG, no matter the molecular weight. The results show that debinding at 60°C is the quickest method of those used for removing 100% of PEG from the parts.

It would be expected that higher temperatures would allow further decreases in removal time, however debinding at 60°C has resulted in a few part defects; in particular, parts with molecular weight PEG 1500. A higher debinding temperature increases the molecular mobility and rate of diffusivity, however debinding at 60°C has proven to be too high as parts have exhibited strength loss, cracking and swelling.⁵³ The higher polymer chain length reduces the PEG's mobility in water, resulting in a disproportion between the penetration of water compared to the diffusion of PEG, ultimately leading to the swelling and cracking exhibited.⁵⁸ Figure 4.21 shows the defects caused to PEG 1500 during water debinding at 60°C.

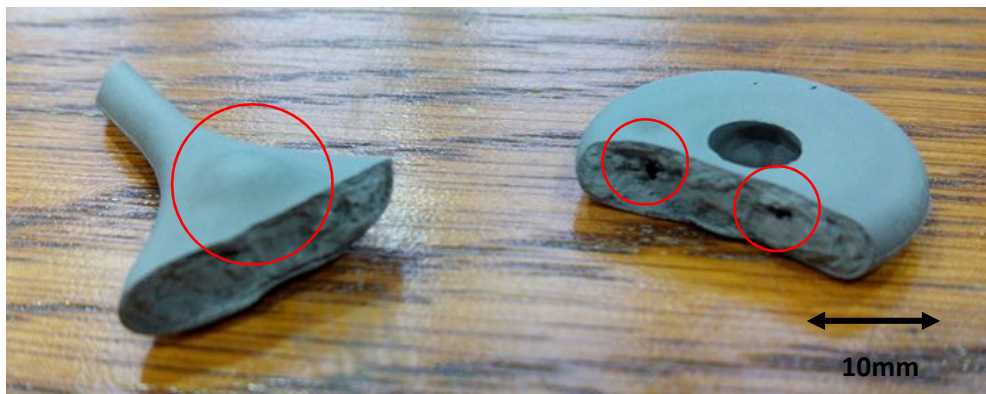


Figure 4.21 Defects caused to PEG 1500 parts during debinding at 60°C

The effect of the molecular weight PEG on debinding time has also been interpreted into a graph, shown in Figure 4.22-4.24. Debinding was carried out on all samples in order to determine the overall weight loss and rate of loss between 0 and 15 hours.

Feedstocks with a higher molecular weight of PEG require a longer debinding time in order to achieve a weight loss of 100%. This is because the polymer chain length is longer and takes longer to break down.

Figure 4.22 The effect of PEG molecular weight on the debinding time at 40°C

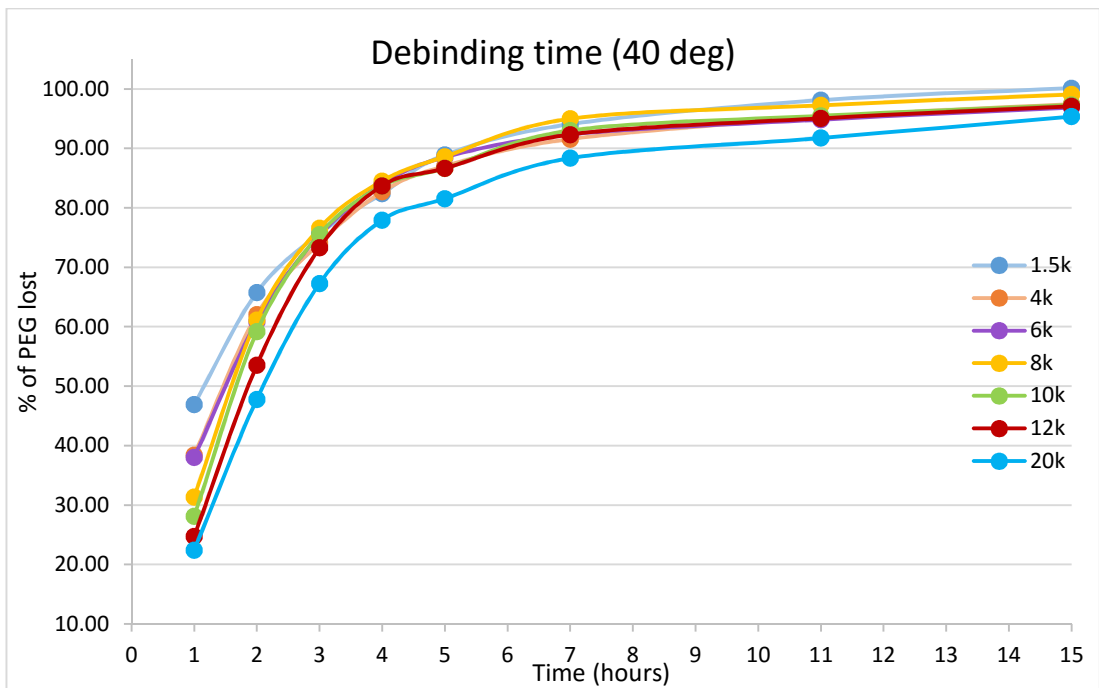


Figure 4.23 The effect of PEG molecular weight on the debinding time at 50°C

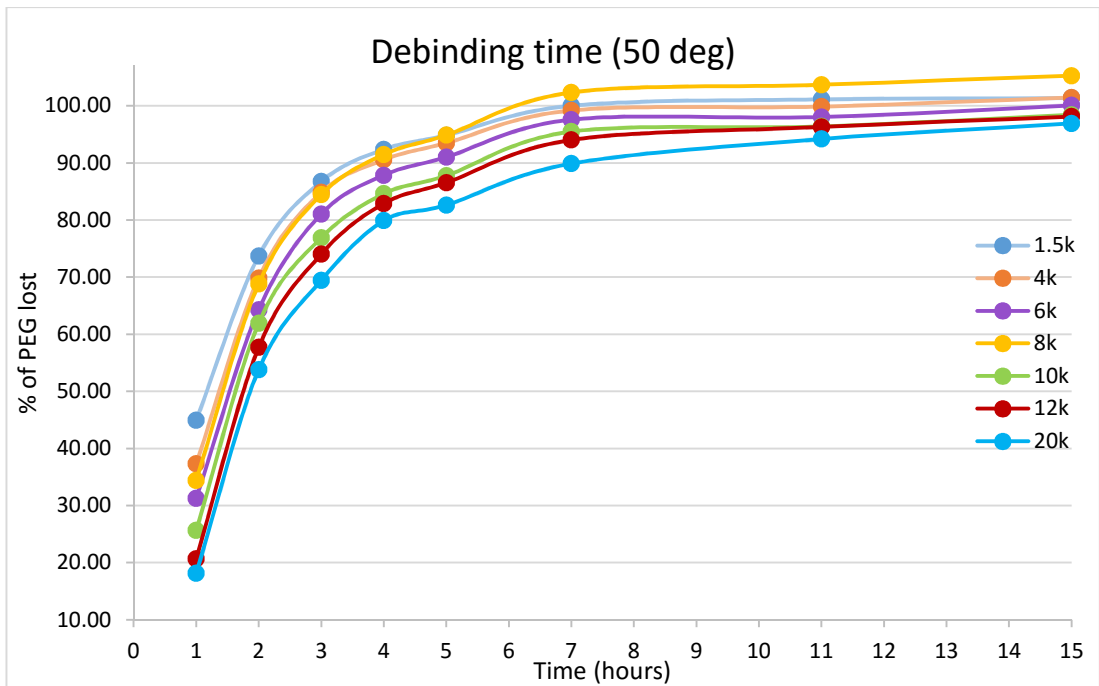
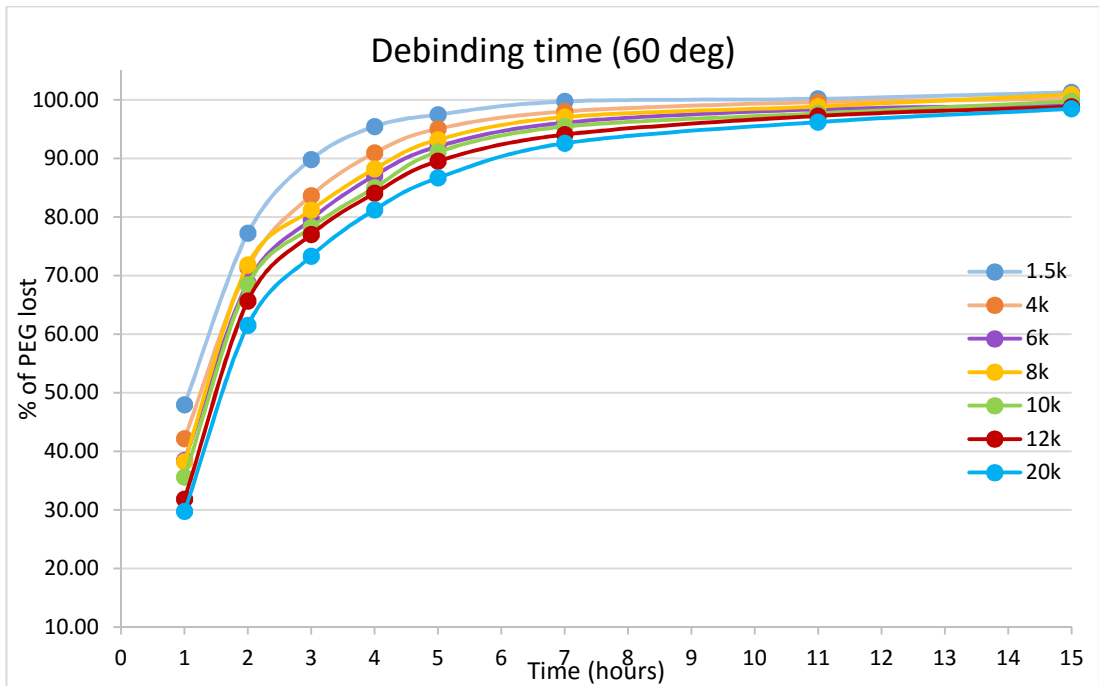


Figure 4.24 The effect of PEG molecular weight on the debinding time at 60°C



By plotting $\ln(1/F)$ against the debinding time, where F is fraction of soluble PEG remaining in the specimen; the mechanism that drives debinding behaviour can be analysed. Figure 4.25 shows this for PEG 1500 debinded at 40°C.

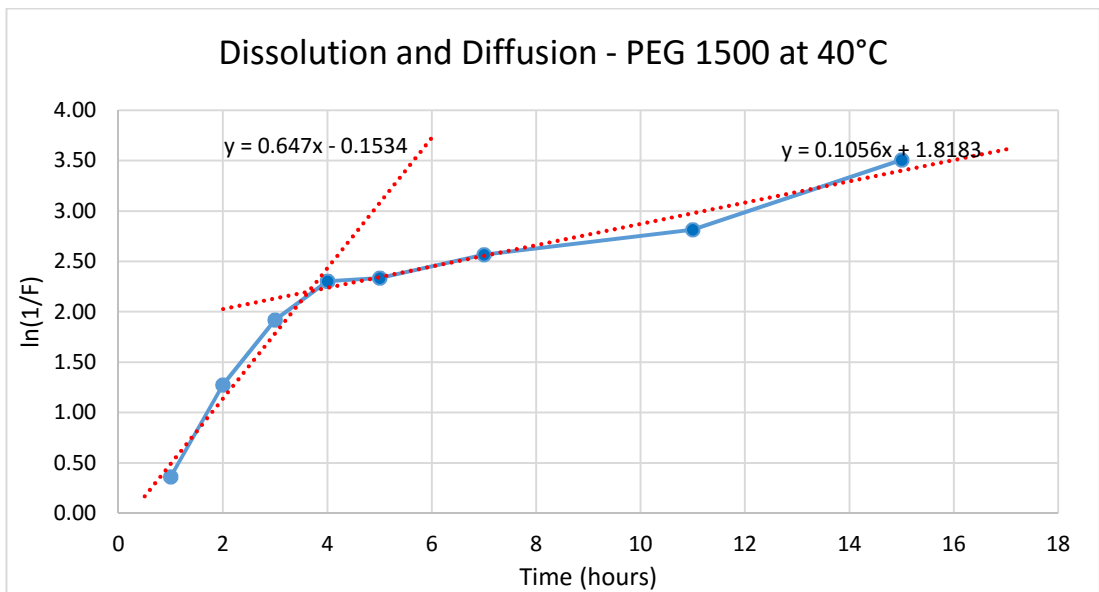


Figure 4.25 $\ln(1/F)$ plot to show two stage debinding mechanism for PEG 1500 at 40°C

As can be seen from Figure 4.25, water debinding is a two stage process, with an initial dissolution phase where the water molecules interact with the PEG at the components surface, before creating a network of pores to then extract PEG by capillary action via diffusion. It can be seen that the dissolution phase lasts for approximately 4 hours for this specific example and the rate of PEG removal is faster than the latter diffusion stage. This is shown by plotting a linear trend line for each stage and evaluating the line gradients. The line gradients for the dissolution and diffusion stages are 0.647 and 0.151 respectively. Therefore the dissolution rate is 4.3 times quicker than the diffusion rate for this specific example.

Both the PEG molecular weight and debinding temperature will have an impact on these two mechanisms.

Figure 4.26 shows the $\ln(1/F)$ plot for PEG 1500 components debinded at different temperatures.

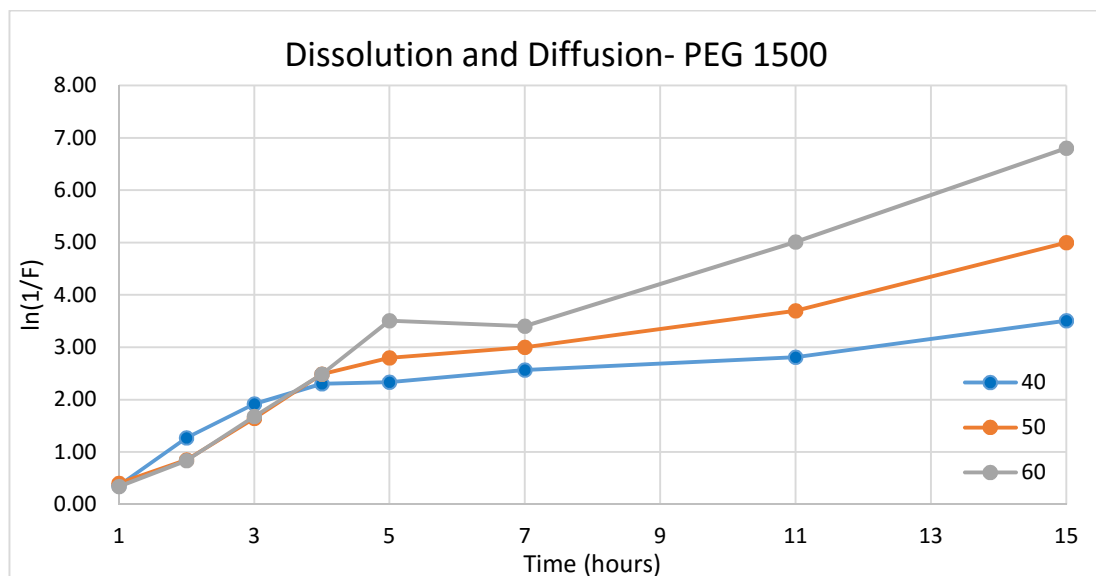


Figure 4.26 $\ln(1/F)$ plot to show two stage debinding mechanism for PEG 1500 increasing water temperatures

It can be clearly seen that the diffusion rate of PEG is increased with a higher water debinding temperature for PEG 1500 at water bath temperatures of 40°C, 50°C and 60°C. The same trend has been found for all PEG molecular weights used in this work.

A closer examination of the dissolution rate (first 4 hours approximately) is shown in Figure 4.27.

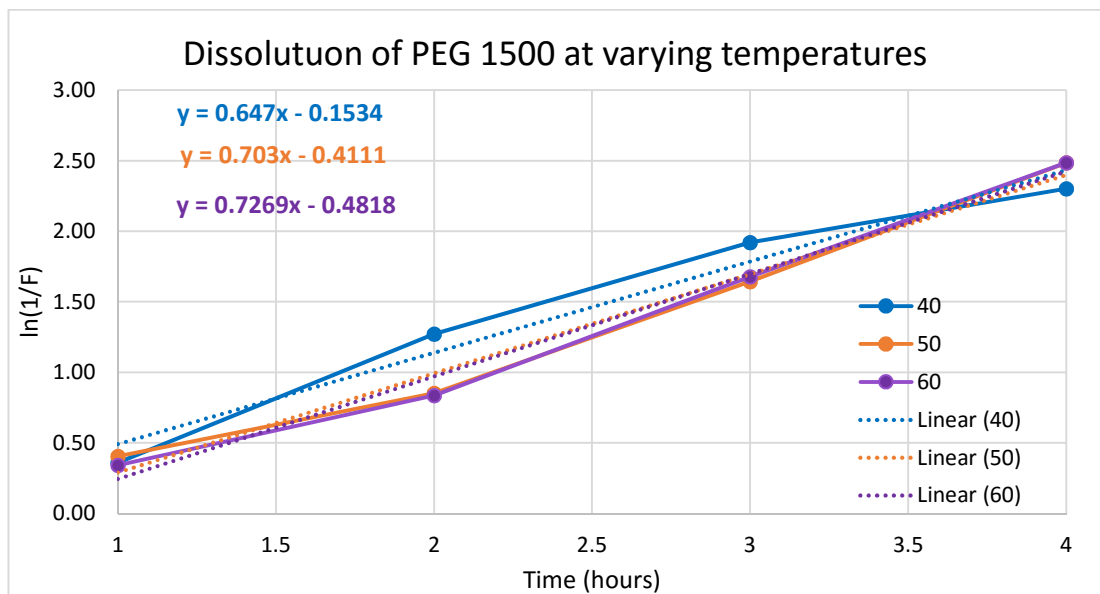


Figure 4.27 $\ln(1/F)$ plot to show dissolution mechanism for PEG 1500 at increasing water temperatures

By looking at the line gradients for the linear trend lines for the dissolution phase of debinding, it is clear that a higher water temperature increases the rate of dissolution for PEG 1500.

Figure 4.28 shows the $\ln(1/F)$ plot for different molecular weight PEGs.

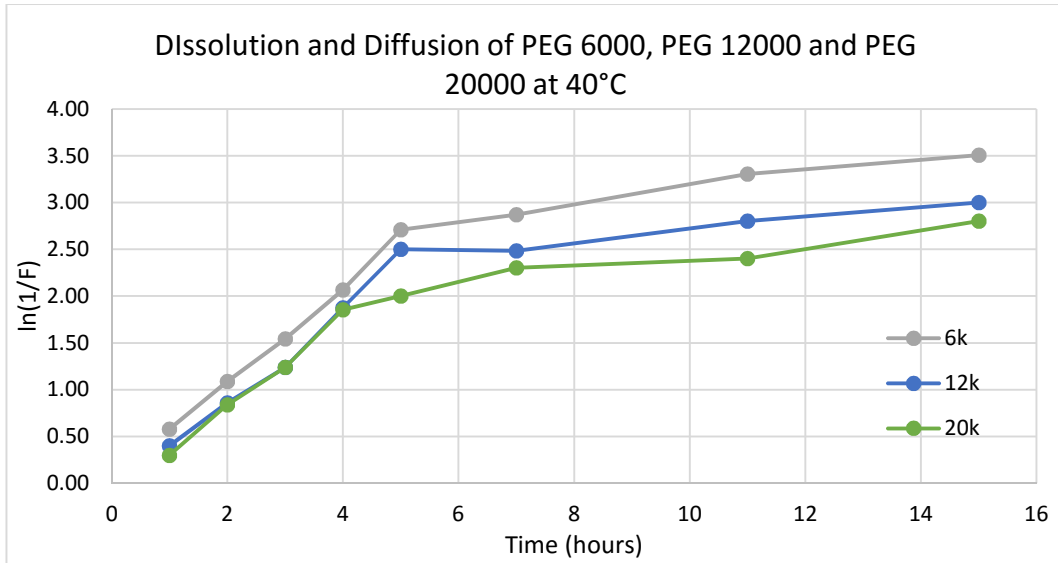


Figure 4.28 $\ln(1/F)$ plot to show dissolution mechanism for PEG 6000, PEG 12000 and PEG 20000 at 40°C

All feedstocks used in this work have exhibited the same debinding behaviour with the two debinding mechanisms of dissolution and diffusion in action.

Table 4.5 Trend line gradient for PEG 6000, PEG 12000 and PEG 20000 for dissolution and diffusion stage of water debinding

Feedstock	Dissolution Gradient (A)	Diffusion Gradient (B)	(A)/(B)
PEG 6000	0.5234	0.0795	6.584
PEG 12000	0.5216	0.079	6.603
PEG 20000	0.4414	0.067	6.588

Table 4.5 shows that the PEG molecular weight has a negative effect on removal rate of PEG in both dissolution and diffusion stages of the water debinding process.

The difference between the dissolution gradients for each feedstock is greater than the difference between the diffusion gradients. This suggests that a lower molecular weight PEG completes the dissolution stage quicker and transitions to diffusion before that of a feedstock with a higher molecular weight of PEG. The decrease in diffusion rates with an increasing PEG molecular weight is less significant.

4.5. Sintering

Following debinding at 40°C, 50°C and 60°C, the tensile bars were dried in an oven for 24 hours at a temperature of 30°C. The parts were then sintered following the process previously outlined in the experimental procedure chapter. The sintering cycle yielded consistent parts, in terms of physical appearance. However the parts that swelled and cracked during debinding at 60°C have cracked further after sintering.

4.6. Dimensional and Density Measurements of Sintered Samples

Table 4.6 outlines the change in dimensions as well as part density for each sintered component. Measurements were taken from three samples and averages of dimensions and density were calculated.

Table 4.6 Average dimensions, shrinkage and density changes after sintering

Feedstock	Moulded		Sintered		Shrinkage		Density after sintering (g/cm ³)	Debinding Temp
	Length (mm)	Thickness (mm)	Length (mm)	Thickness (mm)	% length	% Thickness		
PEG 1500	108.09	3.79	90.06	3.21	16.68	15.32	8.10	40°C
PEG 1500	108.10	3.84	92.55	3.28	14.39	14.56	7.94	50°C
PEG 1500	108.22	3.81	90.68	3.26	16.21	14.43	7.63	60°C
PEG 4000	108.10	3.84	90.49	3.22	16.28	15.98	7.96	40°C
PEG 4000	108.15	3.87	92.82	3.27	14.17	15.66	7.80	50°C
PEG 4000	108.13	3.85	89.77	3.24	16.99	16.00	7.68	60°C
PEG 6000	108.13	3.83	90.77	3.23	16.05	15.68	8.02	40°C
PEG 6000	108.11	3.87	91.79	3.29	15.10	15.15	7.96	50°C
PEG 6000	108.16	3.85	89.52	3.26	17.23	15.40	7.68	60°C
PEG 8000	108.19	3.84	89.94	3.24	16.87	15.64	8.06	40°C
PEG 8000	108.08	3.89	91.92	3.28	14.95	15.52	7.96	50°C
PEG 8000	108.15	3.87	89.77	3.25	16.99	15.86	7.76	60°C
PEG 10000	108.09	3.85	89.99	3.25	16.75	15.65	8.06	40°C
PEG 10000	108.06	3.87	91.92	3.28	14.93	15.23	7.95	50°C
PEG 10000	108.09	3.87	90.24	3.25	16.51	16.09	7.93	60°C
PEG 12000	108.11	3.80	89.81	3.27	16.92	13.93	7.99	40°C
PEG 12000	108.09	3.86	92.09	3.31	14.80	14.09	7.87	50°C
PEG 12000	108.08	3.85	90.48	3.27	16.28	15.06	7.85	60°C
PEG 20000	107.93	3.82	89.89	3.27	16.71	14.31	8.04	40°C
PEG 20000	107.93	3.88	91.77	3.31	14.97	14.78	7.98	50°C
PEG 20000	108.14	3.86	90.93	3.26	15.92	15.47	7.93	60°C

The density measurements taken from the sintered parts vary depending on the debinding temperature used. The bar chart in Figure 4.29 clearly shows there is a trend between debinding temperature and final part density.

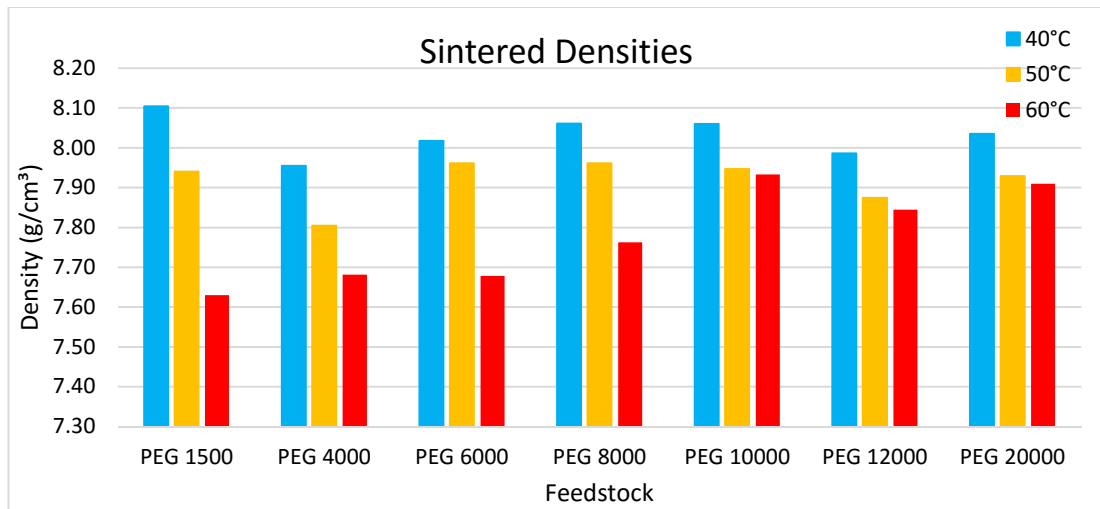


Figure 4.29 Part density after sintering for each debinding temperature

An increased debinding temperature has a significant impact on the part density after sintering, particularly in the feedstocks with a lower molecular weight (PEG 1500 – PEG 8000). The density of the sintered part is lower if the water temperature during debinding is above 40°C. At a higher water temperature, the PEG inside the parts swells during extraction in the water bath as was seen by the part defects in the previous chapter, this results in an increased pore size between metal particles in the part. This has lower impact on the high molecular weight PEG, because of the higher polymer chain length, which reduces the uptake of water by the material and therefore swelling. The polymer requires a greater amount of energy in order to separate the PEG molecules, resulting in less part swelling and a steadier debinding rate.

The theoretical density of Inconel 718 is 8.19 g/cm³. As expected from the MIM process, this density is not achieved. ²⁵ Theoretical density could be achieved through hot isostatic pressing (HIP) of the sintered parts after completion of the MIM process.

There is no clear relationship in dimensional shrinkage after sintering for each feedstock and debinding temperature. Hand held digital callipers were used to measure the dimensions of the parts before and after sintering. Using a more sensitive and accurate piece of equipment could have shown a trend between the different feedstocks or debinding temperatures. The difference in measured sintered density between parts water debinded at different water temperatures would suggest there should also be a dimensional difference between sintered parts.

Figure 4.30 shows the tensile bar development from as moulded, debinded and sintered.



Figure 4.30 Inconel 718 tensile bars for PEG 20000, as moulded (left), debinded (middle) and sintered (right)

4.7. Heat Treatment

At this point of the experimental work it was decided to only proceed with samples debinded at 40°C. These samples had a higher density and it was expected that they would produce better metallography and mechanical testing results. Optimisation of these properties is more important in the final product than reduction in process time.

Heat treatment was carried out in accordance with AMS 5917 -2011 (Metal Injection Moulded Nickel Based Alloy 718 Parts Hot Isostatically Pressed, Solution and Aged) as previously outlined in the Experimental Procedure section of this thesis.

The samples were slightly discoloured due to a small degree of oxidation in the ageing process.

4.8. Dimensional and Density Measurements of Heat Treated Samples

Following the heat treatment process, dimensional checks were carried out on all parts using the same equipment used throughout experiments. There were no measureable dimensional changes from the measurements previously taken after sintering.

Density measurements were also taken as previously described, with no significant change or trend for any of the samples. These results are shown in Table 4.7.

Table 4.7 Inconel 718 density comparison of sintered and heat treated tensile bars using different molecular weight PEG

Feedstock	Sintered density average (g/cm³)	Heat treated density average (g/cm³)
PEG 1500	8.10	8.03
PEG 4000	7.96	7.95
PEG 6000	8.02	8.06
PEG 8000	8.06	8.03
PEG 10000	8.06	8.10
PEG 12000	7.99	7.99
PEG 20000	8.04	8.04

The heat treatment procedure is designed to change the microstructural and mechanical properties of the samples by subjecting them to predetermined temperatures for a long soaking time. The heat treatment was carried out at ambient pressure and the heat profile did not exceed the sintering temperature previously used, therefore there is no driver for the parts to shrink and become denser.

4.9. Microstructure Investigation

The mounted, polished and etched samples in both the as sintered and solution treated condition from each PEG containing tensile bar, were examined using optical microscopy to examine if the PEG molecular weight could have any effect on the microstructure and porosity of the parts.

The pores in each sample appeared fairly round and evenly distributed, with no large irregular voids; this indicates the moulding process has been consistent throughout and the feedstock has been evenly and smoothly injected into the mould. Large voids present under the microscope would indicate the parts have not been fully moulded.

There is little difference or correlation in the appearance of the microstructure across the different samples, indicating the molecular weight of PEG used in the feedstock has no effect on the sintered and heat treated microstructure, if all sintering and heat treatment parameters are kept the same. The measured average grain size also shows little difference or correlation between samples.

Figure 4.31 shows the microstructure and pore distribution for a sample produced from the PEG 20000 feedstock, in both the as sintered and solution treated and aged condition, at different magnifications.

The average grain size, taken from the solution treated and aged micrograph, is very fine, measuring 7.73 μm (average grain size intercept method used).

The microstructure of the solution treated and aged sample consists of particle boundaries that are similar in size and shape of the initial spherical powder used. The dark particles that can be seen at grain boundary triple points are assumed to be precipitates of Inconel 718.

The solution treatment and ageing process has improved the homogeneity of the microstructure; the pores seem to be more evenly distributed, the presence of precipitates at the grain boundaries are more apparent and the grain size is reduced, as compared to the sintered sample.

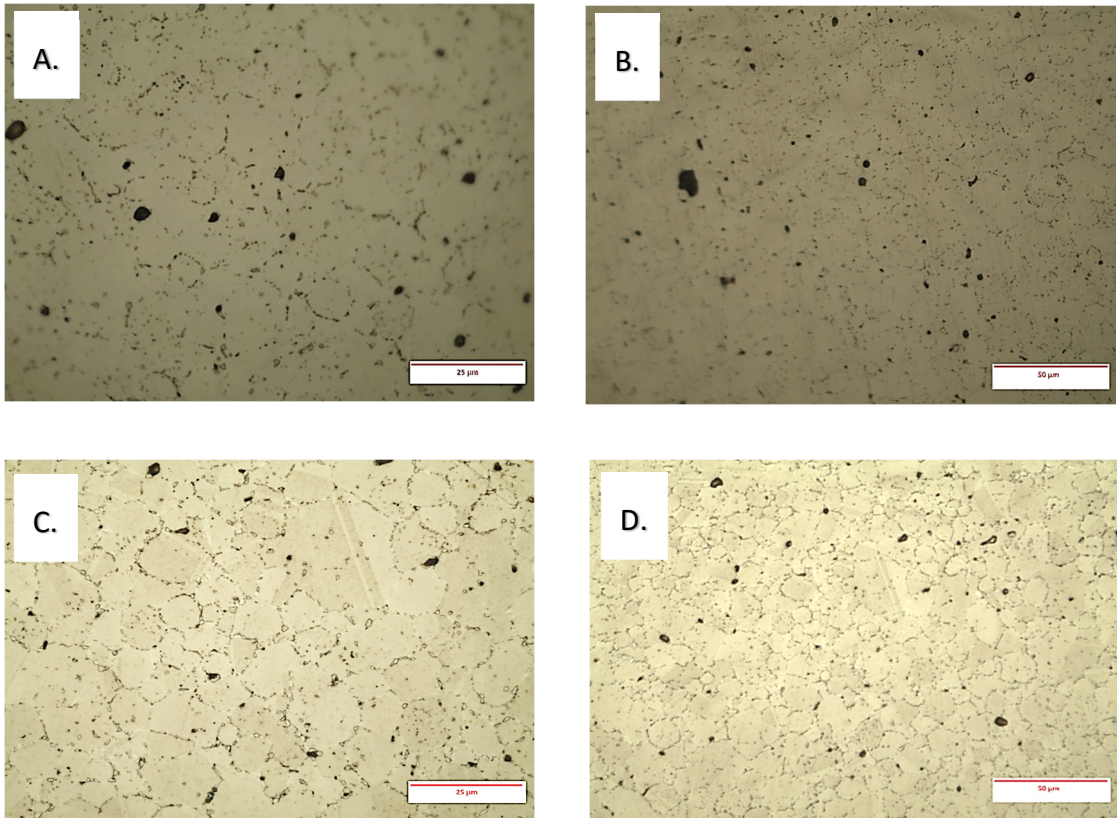


Figure 4.31 Optical micrograph of Inconel 718 PEG 2000 sample; (a) and (b) as sintered, (c) and (d) after solution treatment and ageing as per AMS 5917 -2011.

4.10. Tensile Testing

The tensile testing was carried out as outlined in the previous section of this thesis. Three samples from each feedstock were tested. Each of the parts fractured towards the centre of the gauge length, which indicates there were no significant defects or holes along this length. The fracture surface of each of the parts is clean and flat, with no visible holes or defects at the point of breaking.

The results from the tensile testing of all sintered and heat treated tensile bars debinded at 40°C are shown in Table 4.8 and Figure 4.32. Average values were taken from the three samples tested for each PEG.

Table 4.8 Inconel 718 solution treated and aged mechanical properties of tensile bars

Feedstock	Young's Modulus (GPa)	0.2% P.S. (MPa)	UTS (MPa)	Density
PEG 1500	272.4	947.5	1133.2	8.03
PEG 4000	273.0	968.1	1232.0	7.95
PEG 6000	259.2	954.5	1155.3	8.06
PEG 8000	271.5	952.1	1085.0	8.03
PEG 10000	234.0	938.4	1110.7	8.10
PEG 12000	256.4	944.7	1157.9	7.99
PEG 20000	252.13	969.53	1128.43	8.04

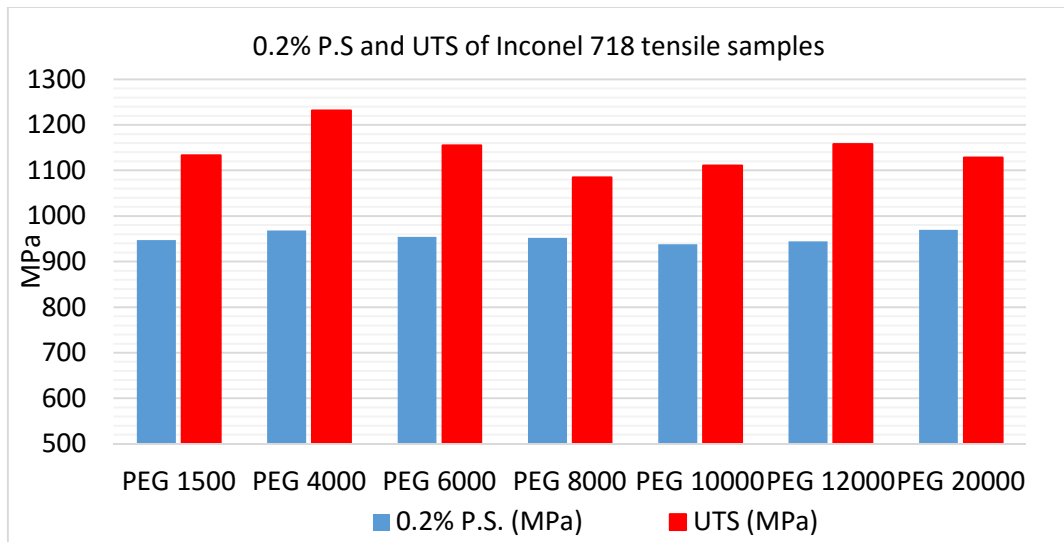


Figure 4.32 0.2% proof stress and ultimate tensile strength of tested samples

It is apparent from the above results that there is no trend in the mechanical properties for the different molecular weight containing feedstocks. There is also no relationship between the part density and the corresponding mechanical properties across the small range of values explored here. This suggests that the molecular weight of PEG is irrelevant after water debinding, as long as the feedstocks are debinded at the same water temperature.

Figure 4.33 shows the mechanical results observed during these experiments in comparison to industrial standards for cast, wrought and MIM standards for Inconel 718. An average of the results from the different PEG containing feedstocks has been taken and represented in the graph.

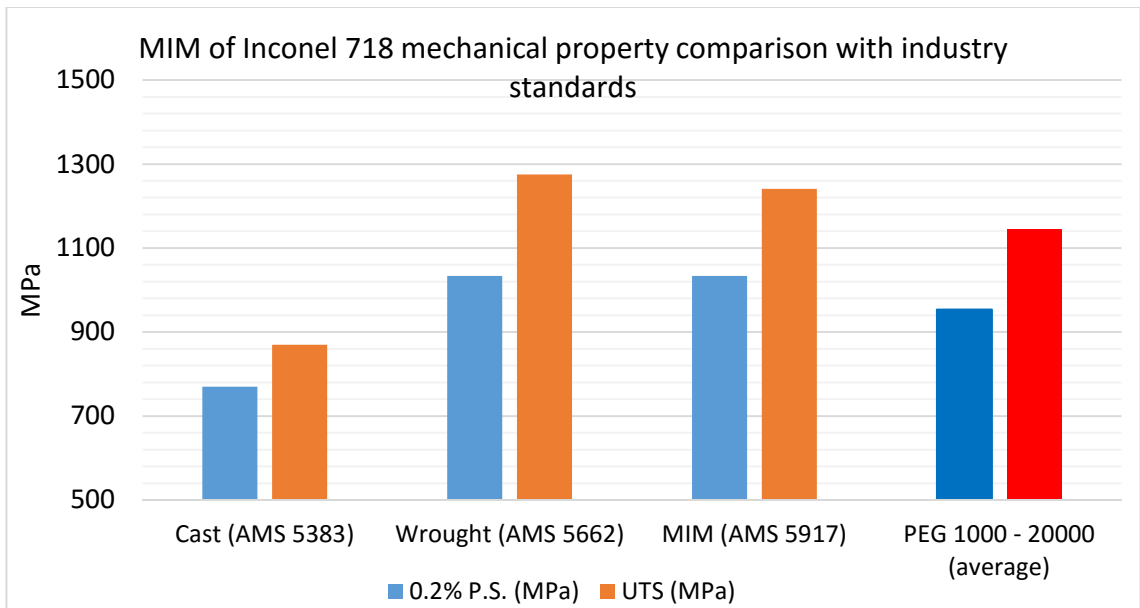


Figure 4.33 MIM of Inconel 718 0.2% P.S and UTS in comparison with industrial standards

The results obtained are superior to the properties for AMS 5383 for cast Inconel 718. This is to be expected as cast parts include a greater size and number of pores and defects, resulting in a lower density. Also the scale of the microstructure in the MIM material compared to cast is finer, originating for the fine powder used. The results are inferior to AMS 5662 for wrought Inconel 718.

The MIM standard AMS 5917 is for sintered, heat treated and HIP'ed test pieces. The results from these experiments are currently inferior to this standard, however a HIP process has not been carried out on the MIM samples, which could significantly increase the mechanical properties.

5. Conclusions

This work has examined the use of MIM of Inconel 718 with different molecular weight PEG components in the binder, assessing the effects on mouldability, debinding rates and temperature and sinterability and resulting mechanical and physical properties.

- The use of a high molecular weight PEG resulted in a higher shear viscosity at higher shear rates during rheology.
- With an increasing molecular weight, flow sensitivity at increasing temperatures decreases.
- During rheology the temperature has little to no effect for any of the feedstocks at a low shear rate, the shear viscosity appears unaffected by change of temperature.
- After injection moulding of tensile bars, there is little variation or correlation between the dimensions and weight measured for each feedstock, denoting the molecular weight of PEG has little or no effect on the dimensions and weight of the moulded part
- An increase in water temperature during debinding has an overall increase on the removal rate of the PEG.
- The higher molecular weight of PEG requires a longer soaking time during debinding, in order to achieve a weight loss of 100%.
- A higher water debinding temperature results in a lower part density after sintering
- There is no clear relationship in dimensional shrinkage after sintering for each feedstock debinded at the same temperature.
- The molecular weight of PEG used in a feedstock has no effect on the microstructure or pore size and distribution when observed under optical microscopy.
- There is no trend observed in the mechanical properties of parts moulded using different molecular weight PEG.
- It can be deduced that the molecular weight of PEG is irrelevant after water debinding, as long as the feedstocks are debinded at the same water temperature.
- The mechanical properties are superior to that of AMS 5383 (cast) and inferior in comparison with AMS 5662 (wrought)
- The mechanical properties are also currently inferior to that of the MIM standard AMS 5917, however further HIP'ing of the components could improve mechanical strength.

6. References

1. Nalbant M, Altın A, Gökkaya H. The effect of cutting speed and cutting tool geometry on machinability properties of nickel-base Inconel 718 super alloys. *Mater. Des.* 2007;28(4):1334-1338. doi:10.1016/j.matdes.2005.12.008.
2. Choudhury I a, El-Baradie M a. Machining nickel base superalloys: Inconel 718. *Proc. Inst. Mech. Eng. Part B J. Eng. Manuf.* 1998;212(3):195-206. doi:10.1243/0954405981515617.
3. Range M, Temperature C. INCONEL alloy 718.
4. Donachie MJ, Donachie SJ. *SUPERALLOYS Second Edition.*; 2002.
5. Contreras JM, Jiménez-Morales A, Torralba JM. Improvement of rheological properties of Inconel 718 MIM feedstock using tailored particle size distributions. *Powder Metall.* 2008;51(2):103-106. doi:10.1179/174329008X313342.
6. Sidambe AT, Derguti F, Russell AD, Todd I. Influence of processing on the properties of IN718 parts produced via Metal Injection Moulding. 2013;7(4):81-85.
7. Latham D. The Sinter Joining of Metal Injection Moulded Components Table of Contents. 2011;(100144990).
8. Davies P. *Metal Injection Moulding of Heat Treated Alloy 718 Master Alloy.*
9. Davies P, Dunstan G, Hayward A, Howells R. Special feature Aerospace adds lustre to appeal of master alloy MIM feedstocks. 2004;(November):14-18.
10. El-bagoury N, Ramadan M. Heat Treatment Effect on Microstructure and Mechanical Properties of Re-Containing Inconel 718 Alloy. 2012;2012(September):924-930.
11. Sago JA, Newkirk JW, Ct J. Author Index THE EFFECTS OF MIM PROCESSING PARAMETERS ON VARIATIONS IN PART WEIGHTS AND DIMENSIONS.
12. Newell M a., Davies H a., Messer PF, Greensmith DJ. Metal injection moulding of scissors using hardenable stainless steel powders. *Powder Metall.* 2005;48(3):227-230. doi:10.1179/174329005X71920.

13. Chuankrerkkul N, Messer PF, Davies H a. Flow and void formation in powder injection moulding feedstocks made with PEG/PMMA binders Part 1 – Experimental observations. *Powder Metall.* 2008;51(1):66-71. doi:10.1179/174329008X271600.
14. Chuankrerkkul N, Messer PF, Davies H a. Flow and void formation in powder injection moulding feedstocks made with PEG/PMMA binders Part 2 – Slip band model. *Powder Metall.* 2008;51(1):72-77. doi:10.1179/174329008X271628.
15. Sidambe a. T, Figueroa I a., Hamilton HGC, Todd I. Metal injection moulding of CP-Ti components for biomedical applications. *J. Mater. Process. Technol.* 2012;212(7):1591-1597. doi:10.1016/j.jmatprotec.2012.03.001.
16. Rao GA, Kumar M, Srinivas M, Sarma DS. Effect of standard heat treatment on the microstructure and mechanical properties of hot isostatically pressed superalloy inconel 718. *Mater. Sci. Eng. A* 2003;355(1-2):114-125. doi:10.1016/S0921-5093(03)00079-0.
17. Yoon TS, Lee YH, Ahn SH, Lee JH, Lee CS. Effects of Sintering Conditions on the Mechanical Properties of Metal Injection Molded 316L Stainless Steel. *ISIJ Int.* 2003;43(1):119-126. doi:10.2355/isijinternational.43.119.
18. Omar MA, Davies HA, Messer PF, Ellis B. The influence of PMMA content on the properties of 316L stainless steel MIM compact. 2001;113:477-481.
19. SAE Aerospace. *AMS 5917-2011-08.*; 2011.
20. GKN. Turbo / Supercharger Components. Available at: <http://www.gkn.com/sintermetals/products/engine/turbo-supercharger-components/Pages/default.aspx>. Accessed March 24, 2014.
21. Standard G. Technical trends Gas atomisation and the economics of blowing hot and cold. 2004;(June):38-41.
22. Hartwig T, Veltl G, Petzoldt F, Kunze H, Schollb R, Kiebackb B. Powders for Metal Injection Molding. 1998;18:1211-1216.
23. García-Escorial a., Lieblich M. Microstructural characterisation of Ni75Al25 and Ni31.5Al68.5 powder particles produced by gas atomisation. *J. Alloys Compd.*

2014;586:S489-S493. doi:10.1016/j.jallcom.2012.10.138.

24. Adames JM. Characterization of polymeric binders for metal injection moulding (MIM). 2007;(Mim).
25. German RM. *Powder Injection Moulding*. New Jersey: Metal Powder Industries Foundation; 1990.
26. Beddow JK. *The Production of Metal Powders by Atomization*. Heydon, London: Technology and Engineering; 1978.
27. Simchi a., Petzoldt F. Cosintering of Powder Injection Molding Parts Made from Ultrafine WC-Co and 316L Stainless Steel Powders for Fabrication of Novel Composite Structures. *Metall. Mater. Trans. A* 2009;41(1):233-241. doi:10.1007/s11661-009-0045-5.
28. Pahat B, Process P. RHEOLOGICAL INVESTIGATION OF WATER ATOMISED STAINLESS STEEL. 2009;4(1):1-8.
29. German RM. Powder Injection Molding Using Water Atomized 316L Stainless Steel. *Int. J. Powder Metall.* 1995;31(3).
30. Persson F. *A Study of Factors Affecting the Particle Size for Water Atomised Metal Powders.*; 2012.
31. Martyn MT, James PJ. The processing of hardmetal components by powder injection moulding. *Int. J. Refract. Met. Hard Mater.* 1993;12:61-69. doi:10.1016/0263-4368(93)90017-A.
32. Asai K. Nippon Seisen Learns from its MIM Experience. *Met. Prog. Report, PM Spec. Featur.* 1993.
33. Park S-J, Wu Y, Heaney DF, Zou X, Gai G, German RM. Rheological and Thermal Debinding Behaviors in Titanium Powder Injection Molding. *Metall. Mater. Trans. A* 2008;40(1):215-222. doi:10.1007/s11661-008-9690-3.
34. Stevenson JF, Roser R, Ilinca F, Dourdour A, Kozlov AS, International H. Table of Contents Author Index Subject Index METAL INJECTION MOLDING : MOLD FILLING

AND PACKING DYNAMICS 2 . National Research Council of Canada Boucherville ,
Quebec J4B 6Y4 Table of Contents Author Index.

35. Song HX, Wu YX, Yuan S, Gong QM, Park S-J, German RM. Mechanical alloying of FeAl intermetallic powder for metal injection moulding process. *Powder Metall.* 2010;53(3):208-212. doi:10.1179/174329009X434275.
36. Ji S, Fan Z, Bevis M. Semi-solid processing of engineering alloys by a twin-screw rheomoulding process. *Mater. Sci. Eng. A* 2001;299(1-2):210-217. doi:10.1016/S0921-5093(00)01373-3.
37. Moballegh L, Morshedian J, Esfandeh M. Copper injection molding using a thermoplastic binder based on paraffin wax. *Mater. Lett.* 2005;59(22):2832-2837. doi:10.1016/j.matlet.2005.04.027.
38. Vervoort PJ, Vetter R, Duszczyc J. Overview of powder injection molding. *Adv. Perform. Mater.* 1996;3(2):121-151. doi:10.1007/BF00136742.
39. Yang W-W, Yang K-Y, Wang M-C, Hon M-H. Solvent debinding mechanism for alumina injection molded compacts with water-soluble binders. *Ceram. Int.* 2003;29(7):745-756. doi:10.1016/S0272-8842(02)00226-2.
40. PolyMIM. Available at: www.polymim.de.
41. Ryer Inc. Available at: www.ryerinc.com.
42. Sigma Aldrich. Poly(ethylene glycol). Available at: <http://www.sigmaaldrich.com/catalog/product/sigma/86101?lang=en®ion=GB>.
43. Sigma Aldrich. Poly(methyl methacrylate). Available at: [http://www.sigmaaldrich.com/catalog/search?interface=All&term=pmma&N=0&mode=match partialmax&focus=product&lang=en®ion=GB](http://www.sigmaaldrich.com/catalog/search?interface=All&term=pmma&N=0&mode=match%20partialmax&focus=product&lang=en®ion=GB).
44. Sigma Aldrich. Stearic Acid. Available at: [http://www.sigmaaldrich.com/catalog/search?interface=All&term=stearic acid&N=0&mode=match partialmax&focus=product&lang=en®ion=GB&cm_re=Did You Mean-_-stearic acid-_-stearic acid](http://www.sigmaaldrich.com/catalog/search?interface=All&term=stearic acid&N=0&mode=match%20partialmax&focus=product&lang=en®ion=GB&cm_re=Did%20You%20Mean%20-%20stearic%20acid%20-%20stearic%20acid).

45. Wen G, Cao P, Gabbitas B, Zhang D, Edmonds N. Development and Design of Binder Systems for Titanium Metal Injection Molding: An Overview. *Metall. Mater. Trans. A* 2012;44(3):1530-1547. doi:10.1007/s11661-012-1485-x.
46. Supati R, Loh NH, Khor KA, Tor SB. Mixing and characterization of feedstock for powder injection molding. 2000;(November):0-5.
47. Omar MA. Dry mixing of feedstock for injection moulding of 316l stainless steel powder. 2004;40:111-120.
48. Winkworth. Z blade sigma mixer. Available at: http://www.mixer.co.uk/winkworth_mixers/z-blade-sigma-mixer.aspx.
49. Ji S. Solidification Behavior and Microstructural Evolution of Near-Eutectic Zn-Al Alloys under Intensive Shear. *Miner. Met. Mater. Soc. ASM Int. 2008* 2008. Available at: <http://link.springer.com/article/10.1007/s11661-008-9713-0/fulltext.html>.
50. ALLROUNDER 270 C GOLDEN EDITION. :1-6.
51. Engenharia E De. Universidade do Minho Escola de Engenharia Hélio Rui Caldeira da Silva Jorge Compounding and Processing of a Water Soluble Binder for Powder Injection Moulding. 2008.
52. Trunec M, Cihlg J. Thermal Debinding of Injection Moulded Ceramics. 1996;2219(96).
53. Chen G., Cao P., Wen G., Edmonds N. Debinding behaviour of a water soluble PEG/PMMA binder for Ti metal injection moulding. *Mater. Chem. Phys.* 2013;139(2-3):557-565. doi:10.1016/j.matchemphys.2013.01.057.
54. Eroglu S, Bakan HI. Solvent debinding kinetics and sintered properties of injection moulded 316L stainless steel powder. *Powder Metall.* 2005;48(4):329-332. doi:10.1179/174329005X66782.
55. MIM B. Beckett MIM - pin and bush. Available at: www.beckettmim.com.
56. TAV. TAV Vacuum Furnaces. Available at: <http://www.tav-altovuoto.it/products.php>. Accessed March 24, 2014.

57. British Standards. Sintered metal materials , excluding hardmetals — Tensile test pieces (ISO. 2009.
58. Hayat MD, Wen G, Zulkifli MF, Cao P. Effect of PEG molecular weight on rheological properties of Ti-MIM feedstocks and water debinding behaviour. *Powder Technol.* 2015;270:296-301. doi:10.1016/j.powtec.2014.10.035.